

# ESTIMATING THE CONDITION NUMBER OF CHEBYSHEV FILTERED VECTORS WITH APPLICATION TO THE CHASE LIBRARY

EDOARDO DI NAPOLI AND XINZHE WU<sup>‡</sup>

**Abstract.** Chebyshev filtered subspace iteration is a well-known algorithm for the solution of (symmetric/Hermitian) algebraic eigenproblems which has been implemented in several application codes [19, 24] or in stand alone libraries [14]. An essential part of the algorithm is the QR-factorization of the array of vectors spanning the active subspace that have been filtered by the Chebyshev filter. Typically such an array has an a-priori unknown high condition number that directly influences the choice of QR-factorization algorithm. In this work we show how such condition number can be bound from above with precise and inexpensive estimates. We then proceed to use these estimates to implement a mechanism for the choice of QR-factorization in the ChASE library. We show how such mechanism enhance the performance of the library without compromising on its accuracy.

**Key words.** Chebyshev polynomials, Subspace Iteration, Filtered vectors, Condition number QR-factorization, numerical accuracy, High-performance Computing.

**1. Introduction.** Subspace iteration with Chebyshev acceleration is among the earliest and most influential iterative techniques developed for computing a selected portion of the spectrum of symmetric (Hermitian) algebraic eigenvalue problems, and it remains a cornerstone of modern large-scale eigensolvers. A trial subspace is first enhanced through a polynomial filtering step that amplifies the components associated with the desired eigenvalues, after which the resulting vectors are orthonormalized and used to construct a reduced eigenvalue problem via a Rayleigh–Ritz projection. This reduced problem is then solved using standard dense diagonalization techniques (e.g., divide-and-conquer algorithm), and the resulting approximate eigenpairs are projected back to the original space and tested for convergence.

From a computational standpoint, this workflow is dominated by two key computations: the filtering step, which can be efficiently expressed as repeated matrix–matrix multiplications (GEMM) and therefore maps well to modern hardware, and the orthonormalization step, which is typically performed using the Householder QR algorithm and constitutes the second most expensive operation. Unlike the filter, Householder QR relies heavily on lower-level BLAS routines and is less amenable to efficient high-performance implementations. A natural alternative is the CholeskyQR algorithm, which is rich in BLAS-3 operations and can be implemented in a manner similar to the Chebyshev filter. However, CholeskyQR is notoriously sensitive to the condition number of the matrix of vectors to be orthonormalized, a difficulty exacerbated by the fact that polynomial filtering tends to produce highly correlated subspaces. Recent variants such as CholeskyQR2 [16] and shifted CholeskyQR2 [15] offer promising alternatives, provided reliable information about the condition number of the subspace is made available. In this work, we present a detailed numerical analysis of the conditioning of the filtered subspace under an exhaustive range of scenarios and show how this information can be exploited to safely modify the orthonormalization step within subspace iteration. We implement the resulting strategy in the ChASE eigensolver library and demonstrate that it delivers both numerical robustness and significant performance gains on modern architectures.

**1.1. Filtered subspace iteration: its inception and modern revival.** One of the the first explicit mention in the scientific literature of subspace iteration applied to the solution of the symmetric algebraic eigenvalue problems is by L. Bauer in 1957 [4]. Following this work, as famously mentioned by Parlett [22], eigensolvers based on subspace iteration [ ... where developed in the 1960s and 1970s when the Lanczos algorithm was under the cloud]. What shaped subspace iteration in its modern form is the fundamental work of Rutishauser in a number of papers spanning from 1969 to 1971 [26–28]. The first paper of this series [26] builds on Bauer’s Simultaneous Iteration method and introduce many of the key ideas included in modern implementations of eigensolvers based on subspace iteration. Soon after is groundbreaking work, Rutishauser published two similar papers with additional details of the algorithm (named *ritzit*) which are at the base of its robustness and efficacy [27, 28].

Soon after Rutishauser’s first publication, several authors contributed to improve his initial algorithm. For instance, the Ritz iteration, which projects the eigenproblem onto the search space using a Jacobi step, was upgraded by Stewart to a Rayleigh-Ritz step so as to avoid to deal with non-positive definite matrices [30]. Stewart rigorously demonstrated the enhanced convergence of the eigenpairs when orthogonal iteration (subspace + orthonormalization) is used in conjunction with Rayleigh-Ritz. Con-

<sup>‡</sup>Jülich Supercomputing Centre, Forschungszentrum Jülich. Wilhelm-Johnen straÙe, 52425–Jülich, Germany. e.di.napoli@fz-juelich.de

currently to these development a version of subspace iteration was developed by civil engineers proposing an algorithm very similar to Rutishauser’s, but their exposition is less clear-cut and uses a language and formalism somewhat different from conventional numerical analysts [7]. The interested reader can find a clear review of the improved *ritzit* algorithm in Parlett book [22].

Alongside these developments, several authors generalized subspace iteration to non-Hermitian and unsymmetric eigenproblems (see [31] for an example). In the intervening years up to the last decade, the development of iterative eigensolvers for the Hermitian eigenvalue problem took a different direction due to the resurgence of the Lanczos algorithm and its variations [8–11, 23, 25, 33, 36]. Subspace iteration eigensolvers saw a revival in popularity starting in the middle of the 2000s with application to electronic structure theory, first in the context of sparse eigenproblems [40, 41], and later also for sequences of dense eigenproblems [5, 20]. This coming back is due in part to the emerging need of solving for just the full subspace without resolving the single eigenpairs [41] and in part to the ability of the eigensolver to receive as input approximate eigenvectors, and in doing so, decrease considerably its time-to-convergence [13].

The last decade has witnessed an increased use of filtered subspace iteration in new advanced methods of electronic structure computations. A Chebyshev filtered subspace iteration has been used to power a discontinuous Galerkin approach to solve the Kohn-Sham equation using a adaptive local basis set [2, 3]. Similarly, an early version of the ChASE library [34] was integrated to solve Excitonic Hamiltonian emerging from the Tamm-Dancoff approximation (TDA) of the Bethe-Salpeter equation [39]. It has been also shown that Chebyshev Filtered subspace returns high-performance gains on many cores [18]. More recently, our team has endeavoured in a substantial effort to develop the ChASE library into a full-fledged accelerated and distributed parallel library [37, 38] with further extensions to pseudo-Hermitian eigenproblems [21] arising from Bethe-Salpeter equation beyond TDA.

**1.2. A modern eigensolver based on Chebyshev Accelerated Subspace iteration.** Let  $A$  be a symmetric or complex Hermitian matrix of size  $n$ , having  $n$  real eigenvalues ordered such that the relation  $\lambda_1 \leq \lambda_2 \leq \dots \leq \lambda_n$  holds. The ascending ordering, which is the opposite of what is traditionally found in the literature, is inspired by application to electronic structure calculations but it is otherwise equivalent to the more common descending ordering description. We are interested in the first  $\text{nev}$  eigenpairs—eigenvalues and their corresponding eigenvectors  $(\lambda_1, x_1), (\lambda_2, x_2), \dots, (\lambda_{\text{nev}}, x_{\text{nev}})$ —for  $\text{nev} \ll n$ . The choice for the wanted part of the eigenspectrum is arbitrary but is in line with the examples presented in this work. Let us just remark that subspace iteration with a polynomial filter can be used equivalently for the highest part of the spectrum and not only to compute the smallest eigenpairs.

---

**Algorithm 1.1** ChASE: Chebyshev Accelerated Subspace iteration Eigensolver

---

**Require:** Matrix  $A$ , (optional) vector matrix  $V^{(0)} \equiv [v_1^{(0)}, \dots, v_{\text{nev}}^{(0)}]$

**Ensure:**  $\text{nev}$  extremal eigenpairs  $(\Lambda, Y)$  with  $\Lambda = \text{diag}(\lambda_1, \dots, \lambda_{\text{nev}})$  and  $Y = [y_1, \dots, y_{\text{nev}}]$ .

- 1: Set the size of search space  $\ell > \text{nev}$
- 2: Initialize  $V^{(0)} \leftarrow \text{randn}(n, \ell)$
- 3: Estimate  $\lambda_1, \lambda_\ell$  and  $\lambda_n$ . ▷ LANCZOS
- 4: **while**  $\text{size}(Y) < \text{nev}$  **do**
- 5:     Filter the vectors,  $V^{(i)} \leftarrow p_{m_i}(A)V^{(i-1)}$ . ▷ CHEBYSHEV FILTER
- 6:     Orthonormalize  $Q^{(i)} \leftarrow [Y V^{(i)}] (R^{(i)})^{-1}$ . ▷ QR ALGORITHM
- 7:     Compute Rayleigh quotient  $\tilde{A} = (Q^{(i)})^H A Q^{(i)}$ . ▷ RAYLEIGH-RITZ (Start)
- 8:     Solve the reduced problem  $\tilde{A}W^{(i)} = W^{(i)}\tilde{\Lambda}^{(i)}$ .
- 9:     Compute  $V^{(i)} \leftarrow Q^{(i)}W^{(i)}$ . ▷ RAYLEIGH-RITZ (End)
- 10:    **for**  $a = \text{converged} \rightarrow \text{nev}$  **do**
- 11:       **if**  $\text{Res}(V_{:,a}^{(i)}, \tilde{\lambda}_a) < \text{TOL}$  **then** ▷ RESIDUALS
- 12:           $\Lambda \leftarrow [\Lambda \ \tilde{\lambda}_a]$
- 13:           $Y \leftarrow [Y \ V_{:,a}^{(i)}]$  ▷ DEFLATION & LOCKING
- 14:       **end if**
- 15:    **end for**
- 16:     $V^{(i)} \leftarrow [V_{:, \text{nonconverged}:\ell}^{(i)}]$
- 17: **end while**

---

The ChASE algorithm Alg. 1.1 is a more sophisticated version of Rutishauser subspace iteration.

The initial input requires only the matrix  $A$  but can also accept a set of vectors  $V^{(0)}$  which span the desired subspace. When specified as input,  $V^{(0)}$  represents approximate solutions (e.g., when solving for a sequence of eigenproblems). When not specified,  $V^{(0)}$  are initialized with normal random vectors (line 2). The order  $\ell$  of  $V^{(0)}$  is such that the search space is larger (but not much larger) than the desired number of eigenpairs `nev`.

In order to work efficiently the Chebyshev filter requires estimates for  $\lambda_1, \lambda_\ell$  and  $\lambda_n$ . Only the latter has to be really bounded from above; the first two numbers can be estimated without compromising the effectiveness of the algorithm. All three values can be provided as part of the input or can be computed by running few Lanczos iterations (line 3). Each time the body of the while loop is repeated, the vectors  $V^{(i)}$  are filtered (line 5) by a Chebyshev polynomial with variable degree  $m_i$ . The resulting vectors are orthonormalized using a QR algorithm (line 6): this is the step which is the focus of this manuscript. The orthonormalization is followed by a Rayleigh-Ritz projection (line 7) at the end of which eigenvector residuals are computed, converged eigenpairs are deflated and locked (line 13) while the non-converged vectors are sent again to the filter to repeat the whole procedure (line 16). This last step ensures that eigenpairs that already satisfy the stopping criterion are not further filtered which would unnecessarily increase the number of floating-point operations (FLOPs) performed by ChASE. Only the remaining non-converged vectors are passed to the filtering step for further refinement.

The orthonormalization phase is a key step of the algorithmic process. In the Hermitian case, ChASE not only orthonormalizes the current search subspace but also ensures orthogonality against all previously converged eigenvectors. This step enhances convergence by removing components of the space that correspond to already converged directions. Consequently, in ChASE, the QR factorization is always applied to a matrix of size  $n \times \ell$  regardless of how many eigenpairs have already converged and been locked. For numerical robustness, this QR factorization is conventionally performed using Householder QR implementation provided by LAPACK or ScaLAPACK. Numerical stability in this step is crucial for the convergence behavior of ChASE, particularly during the initial iterations when the Chebyshev-filtered vectors can be highly correlated. While stability is an important ingredient, the ChASE library pays a price in terms of performance due to the use of a less than ideal algorithm (Householder QR). This is compounded by the observation that the QR factorization becomes increasingly important as more eigenpairs converge and are locked during the iteration process. When computing more than a small fraction of the spectrum, the orthonormalization step can thus become a critical performance bottleneck [37].

**1.3. Replacing Householder QR with Communication-Avoiding CholeskyQR Variants.** On distributed memory architectures, and particularly on GPUs, the traditional Householder QR factorization often becomes a major performance bottleneck. Although Householder QR provides excellent numerical stability, its performance is primarily constrained by communication rather than computation. The algorithm requires frequent synchronization and numerous small data exchanges between processes, especially during panel factorizations. These synchronization points introduce latency that scales poorly with the number of processes and are even more detrimental on GPU-based systems, where the deep memory hierarchy and kernel-launch overheads amplify the cost of fine-grained communication. Consequently, as the number of locked eigenpairs increases in ChASE and the subspace to be orthonormalized grows, the cumulative cost of Householder QR can dominate the overall runtime [37].

To alleviate this bottleneck, we replaced the traditional Householder QR with communication avoiding (CA) variants of CholeskyQR [15, 16], which are more amenable to distributed and GPU-based architectures. In each iteration of ChASE, a QR factorization is performed on a rectangular matrix  $V^{(i)} \in \mathbb{C}^{n \times k}$  with  $n > k$ . Among the available CAQR methods, we favor CholeskyQR over the tall-skinny QR (TSQR) [12], even though both exhibit similar asymptotic communication costs. The main advantage of CholeskyQR lies in its simplicity: it relies on an additive reduction operation, while TSQR requires a QR factorization of a small matrix at every reduction step [16]. This difference simplifies the implementation and improves performance on hierarchical architectures, especially when efficient collective operations such as `MPI_Allreduce` are available. Moreover, TSQR provides a clear performance advantage over ScaLAPACK’s Householder QR primarily when  $n \gg k$  [1], which is not typically the case in ChASE. For instance, in condensed-matter simulations, ChASE often targets about 10% of the spectrum, leading to a moderate rather than an extreme  $n/k$  ratios.

Although CholeskyQR delivers superior performance and scalability, it suffers from a loss of orthogonality when the condition number of  $V^{(i)}$  increases. This loss can be mitigated by performing the procedure twice, yielding the CholeskyQR2 algorithm [16] (see Algorithm 1.2). However, CholeskyQR2

remains limited by the requirement that the Cholesky factorization of the Gram matrix  $R = X^H X$  succeeds, which only holds when the condition number  $\kappa_2(X)$  does not exceed  $\mathcal{O}(\mathbf{u}^{-1/2})$ , where  $\mathbf{u}$  is the unit round-off and  $\kappa_2(X) = \frac{\sigma_{\max}(X)}{\sigma_{\min}(X)}$ .

---

**Algorithm 1.2** CholeskyQR for  $X = QR$ 


---

```

1: function CHOLESKYQR( $X$ , cholDeg)
2:   for  $i = 1, \dots, \text{cholDeg}$  do
3:      $R \leftarrow X^H X$ 
4:      $[R, \text{info}] \leftarrow \text{CHOLESKY}(R)$ 
5:     if  $\text{info} \neq 0$  then
6:       return Failure
7:     end if
8:      $X \leftarrow XR^{-1}$ 
9:   end for
10:  return  $X$ 
11: end function

```

---

To overcome this limitation, Fukaya et al. [15] proposed the shifted CholeskyQR2 (or  $s$ -CholeskyQR2) algorithm, which introduces a preconditioning step that shifts the Gram matrix  $R$  by a small multiple of the identity. This shift effectively reduces the condition number of  $X$ , extending the applicability of CholeskyQR2 to matrices with  $\kappa_2(X)$  up to  $\mathcal{O}(\mathbf{u}^{-1})$ . Table 1.1 summarizes the condition number ranges for each of the QR variants. This characterization enables the dynamic selection of the most appropriate QR factorization variant to balance performance and numerical accuracy.

Table 1.1: Maximal acceptable condition numbers for different QR variants.  $\mathbf{u}$  denotes the unit round-off.

	CholeskyQR	CholeskyQR2	$s$ -CholeskyQR2	HHQR
$\kappa_2(X)$	$\mathcal{O}(1)$	$\mathcal{O}(\mathbf{u}^{-1/2})$	$\mathcal{O}(\mathbf{u}^{-1})$	Any

Given its favorable performance characteristics, employing CholeskyQR and its variants within the ChASE library is highly attractive. At the same time, preserving numerical accuracy is essential and cannot be compromised. Achieving both performance and stability hinges on obtaining a reliable estimate of the condition number of the filtered vectors,  $\kappa_2(V^{(i)})$ . Directly computing this quantity is prohibitively expensive and would negate the performance gains offered by CholeskyQR. In this work, we demonstrate an alternative approach that provides a lightweight yet reliable estimate of the condition number without incurring significant overhead. We first present the resulting strategy and explain how it is used to adapt the QR step within the algorithm. The remainder of the paper is devoted to a rigorous derivation of these results and to numerical experiments that illustrate their impact on both the stability and performance of the ChASE library.

**1.3.1. Condition number estimates and dynamic CAQR.** For the simplest case when ChASE converges in one single step and does not optimize the polynomial degree (one degree for all vectors), we bound the condition number of the filtered vectors  $V^{(i)}$  such that

$$(1.1) \quad \kappa_2(V^{(i)}) \leq \eta |\rho_1|^m,$$

where  $|\rho_1|^m$  is the convergence ratio of the smallest eigenpair (see Definition 2.3). When polynomial degree optimization is enabled, the filtering degree is adapted for each single column of the array  $V^{(i)}$ . In this case, the exponent in  $|\rho_1|^m$  is substituted with the highest polynomial degree which typically corresponds to the last vector of the search space  $m_\ell$ . In the case when vectors are deflated and locked the expression for the bound gets further modified to

$$(1.2) \quad \kappa_2(V^{(i)}) \lesssim \eta |\rho_{k+1}|^{m_{k+1}} |\rho_1|^{m_\ell - m_{k+1}}.$$

where  $m_k$  is the Chebyshev polynomial degree corresponds to the Ritz pair of index  $k$ , and  $V^{(i)} \leftarrow [Y V^{(i)}]$  is the rectangular matrix to be factorized, including the converged eigenvectors  $Y$  and newly filtered subspace.

These estimations rely solely on data already available within ChASE—namely, the spectral bounds  $(c, e)$ , the computed Ritz values  $\Lambda$ , the optimized filter degrees  $m_i$ , and the number of locked eigenpairs  $k$ . As already mentioned, these estimations are based on a detailed spectral analysis of the Chebyshev-filtered subspace and constitute the central contribution of this paper which is exposed in the following sections. Based on the estimated condition number Eqs. (1.1) and (1.2), we select the appropriate CholeskyQR variant following the heuristic in Algorithm 1.3. For double precision, if the estimated condition number exceeds  $10^8$ , the  $s$ -CholeskyQR2 variant is employed. For small condition numbers (below 20), standard CholeskyQR suffices, while intermediate cases use CholeskyQR2. For robustness, a fallback mechanism (Algorithm 1.3, line 8) ensures that any failure in  $s$ -CholeskyQR2 safely reverts to ScaLAPACK’s Householder QR routine.

---

**Algorithm 1.3** Dynamic CAQR selection in ChASE

---

```

1: function DYNAMIC-CAQR( $X$ , estCond)
2:   if estCond >  $10^8$  then                                     ▷ High condition number: use  $s$ -CholeskyQR2
3:      $R \leftarrow X^H X$ 
4:     norm  $\leftarrow \|X\|_F$ 
5:      $s \leftarrow 11(mn + n(n + 1)) \mathbf{u}$  norm
6:     [ $R$ , info]  $\leftarrow$  CHOLESKY( $R + sI$ )
7:     if info  $\neq$  0 then                                       ▷ Cholesky failed, fallback to Householder QR
8:        $X \leftarrow$  HOUSEHOLDERQR( $X$ )
9:     else
10:       $X \leftarrow XR^{-1}$ 
11:       $X \leftarrow$  CHOLESKYQR( $X$ , cholDeg = 2)
12:    end if
13:  else if estCond < 20 then                                     ▷ Well-conditioned: use single CholeskyQR
14:     $X \leftarrow$  CHOLESKYQR( $X$ , cholDeg = 1)
15:  else                                                         ▷ Moderate conditioning: use CholeskyQR2
16:     $X \leftarrow$  CHOLESKYQR( $X$ , cholDeg = 2)
17:  end if
18:  return  $X$ 
19: end function

```

---

In section 2, we describe the spectral properties of the filtered vectors  $V^{(i)}$  both in the case of generic polynomial degree and when such a degree is optimized for each single filtered vector. Section 3 provides a numerical analysis of the bounds for  $\kappa_2(V^{(i)})$  in all possible cases. Section 4 is devoted to numerical tests of the condition number bounds, comparison of dynamic CAQR with the traditional QR decomposition and some scaling tests. In section 5 we summarize and conclude.

**2. Spectral decomposition of the subspace filtered by Chebyshev polynomials.** In this section, we present a formal characterization of the subspace formed by vectors after the application of the filtering process. We begin by recalling the asymptotic properties of Chebyshev polynomials and then describe how these polynomials are employed to filter a matrix of vectors. Next, we introduce the notion of the convergence ratio associated with each eigenpair and demonstrate how these ratios naturally appear in the spectral decomposition of the filter. This framework allows us to express the filtered vectors through a matrix decomposition that clearly separates the components associated with the desired portion of the spectrum from those corresponding to the undesired part.

**2.1. Chebyshev polynomials and their asymptotic properties.** In order to address the general convergence properties of the Chebyshev acceleration of the subspace iteration algorithm, let us briefly recall the definition of the Chebyshev polynomials of the first kind and briefly describe their asymptotic properties.

DEFINITION 2.1 (Chebyshev Polynomials). *The Chebyshev Polynomials  $C_m(t)$  of degree  $m$  on the interval  $[-1, 1]$  are defined as*

$$(2.1) \quad C_m(t) = \cos(m \cos^{-1}(t)), \quad |t| \leq 1$$

*The domain of definition can be extended to the entire real axis by*

$$C_m(t) = \cosh(m \cosh^{-1}(t)), \quad t \in \mathbb{R}$$

It customary and more practical to compute Chebyshev polynomials through a 3-terms recurrence relation, which can be easily derived from Prosthaphaeresis formula for the sum of two cosines (generalized to hyperbolic cosine using the Osborn's rule)

$$(2.2) \quad C_{m+1}(t) = 2tC_m(t) - C_{m-1}(t) \quad \forall t \in \mathbb{R}.$$

This recurrence relation together with the direct computation of  $C_0(t) = 1$  and  $C_1(t) = t$  from eq. (2.1) implies the Chebyshev Polynomials of any degree  $m$  are indeed polynomials in  $t$  whose maximal degree is  $m$ . While on the interval  $[-1, 1]$  a polynomial of degree  $m$  reproduces an oscillating function with  $m - 1$  extrema, for  $|t| > 1$  the function diverges quite rapidly already for modest values of  $m$ . This behavior can be easily quantified by expressing  $C_m(t)$  as an implicit function of  $t$ . Let us define  $\rho \doteq \exp(y)$ , and write  $\cosh(y) = \frac{\rho + \rho^{-1}}{2} = t$ , we obtain

$$\rho^2 - 2t\rho + 1 = 0 \quad \Rightarrow \quad \rho = t \pm \sqrt{t^2 - 1},$$

which implies that both  $\rho$  and  $\rho^{-1}$  are admissible solutions. By convention we choose

$$|\rho| = \max_{\{\pm\}} \left| t \pm \sqrt{t^2 - 1} \right|, \quad |\rho|^{-1} = \min_{\{\pm\}} \left| t \pm \sqrt{t^2 - 1} \right| \quad \text{for } |t| > 1$$

plug back in the definition of  $\rho$  in order to express  $y$

$$y = \cosh^{-1}(t) = \ln |\rho|.$$

Now the polynomial can be re-written as

$$(2.3) \quad C_m(t) = \cosh(m \ln |\rho|) = \frac{|\rho|^m + |\rho|^{-m}}{2}.$$

Since  $|\rho|$  is, by definition, always bigger than one, the leading asymptotic behavior of the polynomial for  $|t| > 1$  is given by  $C_m(t) \sim \frac{|\rho|^m}{2}$ . In other words outside of the interval  $[-1, 1]$ ,  $C_m(t)$  diverges as a polynomial of degree  $m$ . Incidentally inside this interval, the full expression for  $C_m(t)$  is still valid. The only difference is that now  $\rho$  assumes complex values and so does the inverse hyperbolic function

$$\rho = t \pm i\sqrt{1 - t^2} \quad \Rightarrow \quad \cosh^{-1}(t) = \arg(t \pm i\sqrt{1 - t^2}) = y,$$

where  $y$  is nothing else than the angle corresponding to a point on a circle of unit radius in the complex plane. Then eq. (2.3) now indicates the maximum value of  $C_m(t)$  for  $|t| < 1$ , namely 1. The following theorem [29] provides the base for the Chebyshev acceleration of subspace iteration.

**THEOREM 2.2.** *Let  $|\gamma| > 1$  and  $\mathbb{P}_m$  denote the set of polynomials of degree smaller or equal to  $m$ . Then the extremum*

$$\min_{\{p \in \mathbb{P}_m, p(\gamma)=1\}} \max_{\{t \in [-1, 1]\}} |p(t)|$$

is reached by

$$p_m(t) \doteq \frac{C_m(t)}{C_m(\gamma)}.$$

In plain words, let's fix a point  $\gamma$  and consider all polynomials which go through this point and which are maximal on a certain interval that does not contain  $\gamma$ . The smaller of these polynomials is uniquely realized by  $p_m(t)$ . Without affecting the theorem statement, the definition of  $p_m(t)$  can be extended to generic  $t$  but for our purpose it is most useful for  $|\gamma| \geq |t| \geq 1$ .

This polynomial can be straightforwardly generalized to a generic interval  $x \in [\alpha, \beta] \subset \mathbb{R}$ . The following linear transformation  $t(x) = \frac{x-c}{e}$  maps the interval  $[\alpha, \beta]$  onto  $[-1, 1]$  where  $c = \frac{\alpha+\beta}{2}$  define the center of the interval and  $e = \frac{\beta-\alpha}{2}$  its half-width. For large  $m$  the leading order of  $p_m(x)$  is then

$$(2.4) \quad \lim_{m \rightarrow \infty} p_m(x_t) \doteq \frac{C_m\left(\frac{x_t-c}{e}\right)}{C_m\left(\frac{x_\gamma-c}{e}\right)} \sim \frac{|\rho_{x_t}|^m}{|\rho_{x_\gamma}|^m} \quad \text{with} \quad |\rho_{x_\gamma}| = \max_{\{\pm: x_\gamma \notin [\alpha, \beta]\}} \left| \frac{x_\gamma - c}{e} \pm \sqrt{\left(\frac{x_\gamma - c}{e}\right)^2 - 1} \right|.$$

When  $x \in [\alpha, \beta]$  the asymptotic limit simplifies to  $p_m(x) \sim \frac{1}{|\rho_{x_\gamma}|^m}$  since  $\sup_{x \in [\alpha, \beta]} |\rho_x| = 1$ . This asymptotic behavior is crucial for the use of such polynomials as accelerators of the subspace iteration.

**2.2. Filtering vectors with Chebyshev polynomials.** Theorem 2.2 provides the base on which to build a Chebyshev polynomial filter which enhances the convergence of the standard subspace iteration eigensolver. Initial input vectors  $V$  are filtered exploiting the 3-terms recurrence relation written implicitly as a function of the action of  $A$  on the vectors  $V$

$$(2.5) \quad C_m(V) = 2 A C_{m-1}(V) - C_{m-2}(V) \quad ; \quad C_m(V) \stackrel{\text{def}}{=} C_m(A) \cdot V.$$

A polynomial filter improves the subspace iteration by manipulating the initial subspace in such a way that the components in the unwanted part of the spectrum relative to those in the wanted part are dramatically suppressed. This is graphically illustrated in Figure 2.1 where the part of the eigenspectrum in red is mapped to the interval  $[-1, 1]$  and corresponds to the unwanted part of the spectrum.

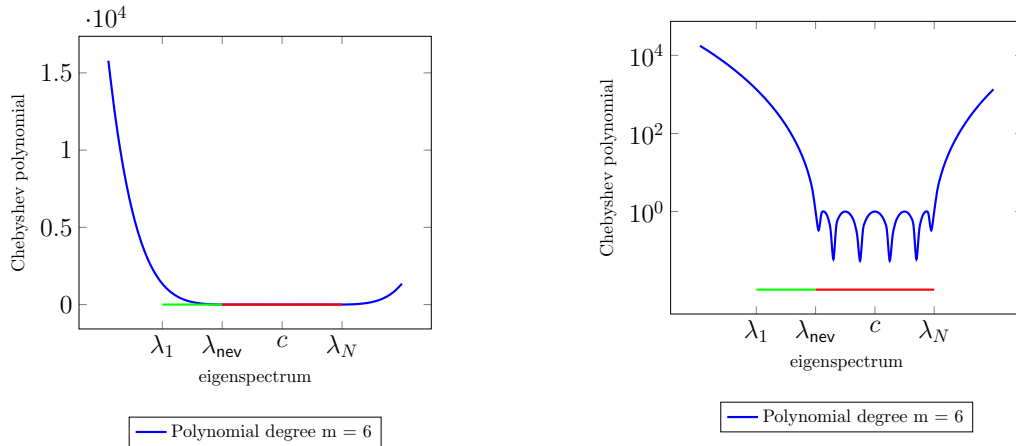


Fig. 2.1: Schematic use of the Chebyshev polynomial  $C_m(\lambda)$  to enhance the components  $V$  aligned to the eigenvectors corresponding to the desired portion of the spectrum  $[\lambda_1, \lambda_{\text{nev}}]$  (in green) of an Hermitian matrix  $A$ . Conversely the components of  $V$  aligned with eigenpairs in the interval  $[\lambda_{\text{nev}}, \lambda_N]$  (in red) are suppressed. Here  $\lambda_N$  indicates the largest eigenvalue of  $A$ .

A value that quantify the amount of filtering operated by the Chebyshev polynomial is the convergence ratio defined through the variable  $|\rho_a|$  where  $a$  is the index of the eigenvalues outside of the interval  $[\alpha, \beta]$ .

DEFINITION 2.3. *The **convergence ratio** for the eigenvector corresponding to eigenvalue  $\lambda_a$  is defined as*

$$\tau(\lambda_a) = |\rho_a|^{-1} = \min_{\{\pm: \lambda_a \notin [\alpha, \beta]\}} \left| \frac{\lambda_a - c}{e} \pm \sqrt{\left(\frac{\lambda_a - c}{e}\right)^2 - 1} \right|.$$

The further away  $\lambda_a$  is from the interval  $[\alpha, \beta]$  the larger is  $|\rho_a|$  and the faster any filtered vector  $v \in V$  should converge to the eigenvector  $x_a$  corresponding to eigenvalue  $\lambda_a$ . In practice the statement that  $|\rho_a|^{-1}$  represents the convergence ratio of  $v$  is more a rule of thumb than a precise statement: a rigorous demonstration requires a substantial effort and it is not in the scope of this paper and our results do not depend on it. What is important to keep in mind is that  $\forall \lambda_a \notin [\alpha, \beta], |\rho_a| > 1$ .

When dealing with numerical implementation of Chebyshev acceleration,  $p_m(\lambda) = \frac{C_m(\frac{\lambda_a - c}{e})}{C_m(\frac{\lambda_1 - c}{e})}$  is actually computed using the 3-term recurrence relation of eq. (2.5) for the action of the numerator of  $p_m(A)$  on the vectors  $V$ . The calculation of the constant denominator  $\eta_m \doteq C_m(\frac{\lambda_1 - c}{e})$  is carried out separately from to the matrix numerator. By naming  $\sigma_{m+1} \doteq \frac{\eta_m}{\eta_{m+1}}$  it is possible to recursively define  $\sigma_m$

$$(2.6) \quad \sigma_m = \frac{1}{\frac{2}{\sigma_1} - \sigma_{m-1}} \quad \text{with} \quad \sigma_1 = \frac{\eta_0}{\eta_1} = \frac{e}{\lambda_1 - c}.$$

With this definition in hand, the action of  $p_m(A)$  on  $V$  can be expressed as a specialized 3-term recurrence

relation

$$\begin{aligned}
p_m(A)V &= \frac{C_m\left(\frac{A-cI}{e}\right)}{\eta_m}V \\
&= \frac{2\frac{A-cI}{e}C_{m-1}\left(\frac{A-cI}{e}\right) - C_{m-2}\left(\frac{A-cI}{e}\right)}{\eta_m}V \\
&= 2\frac{A-c}{e}\frac{\eta_{m-1}}{\eta_m}\frac{C_{m-1}\left(\frac{A-cI}{e}\right)}{\eta_{m-1}}V - \frac{\eta_{m-1}}{\eta_m}\frac{\eta_{m-2}}{\eta_{m-1}}\frac{C_{m-2}\left(\frac{A-cI}{e}\right)}{\eta_{m-2}}V \\
&= 2\frac{A-cI}{e}\sigma_m p_{m-1}(A)V - \sigma_m\sigma_{m-1}p_{m-2}(A)V.
\end{aligned}$$

In practical terms, the polynomial filter above is realized iteratively as illustrated in Algorithm 2.1.

---

**Algorithm 2.1** Chebyshev polynomial filter

---

**Require:** Matrix  $A$ , random vector  $V$  and eigenvalue estimates  $\tilde{\lambda}_1$  and  $\tilde{\lambda}_{\text{nev}}$ .

**Ensure:** Filtered vectors  $V^{(m)}$ .

$$c = \frac{\tilde{\lambda}_1 + \tilde{\lambda}_{\text{nev}}}{2}, \quad e = \frac{\tilde{\lambda}_{\text{nev}} - \tilde{\lambda}_1}{2}, \quad \sigma_1 = \frac{e}{\tilde{\lambda}_1 - c};$$

$$V^{(1)} = \frac{\sigma_1}{e}(A - cI_n)V;$$

**for**  $i = 2 \rightarrow m$  **do**

$$\sigma_i = \frac{1}{\frac{2}{\sigma_1} - \sigma_{i-1}};$$

$$V^{(i)} = \frac{2\sigma_i}{e}(A - cI_n)V^{(i-1)} - \sigma_{i-1}\sigma_i V^{(i-2)};$$

**end for**

---

As mentioned above, it can be shown that the component of the random array of vectors  $V$  converges to the subspace spanned by the eigenvectors  $x_a$  corresponding to  $\lambda_a \notin [\alpha, \beta]$  with a  $\tau_a$  convergence ratio. Roughly speaking, this observation implies that each vector  $v_a \in V$  could in theory be filtered with a polynomial degree just high enough to ensure the convergence to  $x_a$  within a specific threshold. In the ChASE library this mechanism is implemented using a polynomial degree  $m$  which is an ordered array of degrees with the same dimension of  $V$  instead of just one value for all. Algorithm 2.1 for loop is then slightly modified with  $m \rightarrow m_a$  and the addition of an if statement that stops filtering vectors  $v_a$  as soon as  $m_a < i$ . The resulting algorithm optimizes for the minimum number of operations necessary to reach convergence.

**2.3. Spectral decomposition of the filtered vectors.** In this section we provide a simple spectral decomposition of  $p_m(A)V$  which will then be used to derive some of the results on the condition number estimate of  $p_m(A)V$  in the following sections. Using the spectral decomposition of  $A = X\Lambda X^H$ , let us represent the set of initial vectors  $V^{(0)}$  by projecting them over the exact eigenvectors  $X = (X_\ell X_3)$  which are respectively of order  $\ell$ , and  $n - \ell$

$$V^{(0)} \equiv X X^H V^{(0)} = X_\ell S_\ell + X_3 S_3$$

where  $S_\ell \in \mathbb{C}^{\ell \times \ell}$ , and  $S_3 \in \mathbb{C}^{(n-\ell) \times \ell}$  (see [32]). We want to emphasize here that the subspace of size  $\ell$  can be further split in two subspaces  $X_\ell = (X_1 X_2)$  with corresponding matrix of coefficients  $S_1$  and  $S_2$  with  $S_1 \in \mathbb{C}^{k \times \ell}$ , and  $S_2 \in \mathbb{C}^{(\ell-k) \times \ell}$ . This further subdivision is not used in the spectral representation below but it is useful to emphasize the difference between the subspace corresponding to the first  $\text{nev}$  eigenvalues and the remaining  $\text{nextra}$  in ChASE. In this paper such subdivision will also be useful when the considering the estimation of the condition number bound when some of the vectors are locked and deflated (see Sec. 3.3). Let us temporarily drop the superscript index of  $V$  and consider such decomposition for the vectors outputted by the filter (see line 5 of the algorithm 1.1) at a generic ( $i$ ) iteration in the case of constant degree  $m$

$$(2.7) \quad p_m(A)V = X_\ell \Gamma_\ell^m S_\ell + X_3 \Gamma_3^m S_3$$

where the diagonal matrices  $\mathfrak{p}_m(\Lambda_\ell) \doteq \Gamma_\ell^m \in \mathbb{C}^{\ell \times \ell}$ , and  $\mathfrak{p}_m(\Lambda_3) \doteq \Gamma_3^m \in \mathbb{C}^{(n-\ell) \times (n-\ell)}$ . Even for moderately small values of  $m$  these matrices are positive definite and so invertible. Unless the choice of vectors  $V^1$  is quite pathological, we can also safely assume that  $S_\ell$  is of maximal rank and so invertible.

The expression (2.7) for  $\mathfrak{p}_m(A)V$  can be further manipulated so as to make a clear distinction between the desired subspace spanned by  $X_\ell$  and the rest,

$$(2.8) \quad \mathfrak{p}_m(A)V = \left( X_\ell + X_3 \Gamma_3^m S_3 (S_\ell)^{-1} (\Gamma_\ell^m)^{-1} \right) \Gamma_\ell^m S_\ell.$$

The  $\Gamma$ -matrices are diagonal and, already for moderately small values of  $m$ , have the simple expressions

$$(2.9) \quad \begin{aligned} \Gamma_\ell^m &= |\rho_1|^{-m} \times \text{diag}(|\rho_1|^m, |\rho_2|^m, \dots, |\rho_\ell|^m) \\ (\Gamma_\ell^m)^{-1} &= |\rho_1|^m \times \text{diag}(|\rho_1|^{-m}, |\rho_2|^{-m}, \dots, |\rho_\ell|^{-m}) \\ \Gamma_3^m &= |\rho_1|^{-m} \times I. \end{aligned}$$

As illustrated at the end of Section 2.2, in the case of degree optimization the polynomial degree  $m$  is not an integer anymore but an array of integers  $m = (m_1, m_2, \dots, m_\ell)$ , one for each of the column vectors of  $V$ , with  $m_1 \leq m_2 \leq \dots \leq m_\ell$ . The expression  $\mathfrak{p}_m(A)V$  then generalizes to signify

$$\mathfrak{p}_m(A)V \equiv (\mathfrak{p}_{m_1}(A)v_1, \mathfrak{p}_{m_2}(A)v_2, \dots, \mathfrak{p}_{m_\ell}(A)v_\ell),$$

where  $V \equiv (v_1, v_2, \dots, v_\ell)$ , with  $v_a \in \mathbb{C}^n$ . Despite the apparent complication,  $\mathfrak{p}_m(A)V$  can still be expressed through  $\Gamma$  matrices with the only difference that their expression in terms of the inverse of the ratio of convergence is modified to

$$(2.10) \quad \begin{aligned} \Gamma_\ell^m &= \text{diag}\left(1, \frac{|\rho_2|^{m_2}}{|\rho_1|^{m_2}}, \dots, \frac{|\rho_\ell|^{m_\ell}}{|\rho_1|^{m_\ell}}\right) \\ (\Gamma_\ell^m)^{-1} &= \text{diag}\left(1, \frac{|\rho_1|^{m_2}}{|\rho_2|^{m_2}}, \dots, \frac{|\rho_1|^{m_\ell}}{|\rho_\ell|^{m_\ell}}\right) \\ \Gamma_3^m &= |\rho_1|^{-m_\ell} \times I. \end{aligned}$$

**2.3.1. The case of locked and deflated vectors.** In the ChASE library, as in any realization of the subspace iteration algorithm, all the steps from the filtering to the convergence check are repeated within a loop. When checking for convergence, each vector that has a residual below threshold is locked and deflated out of  $V$  (see Algorithm 1.1). In this case, the spectral decomposition of the vectors to be re-orthogonalized takes a different structure that needs to be further analyzed.

Without loss of generality, let us start from the the assumption that at a certain iteration  $k$  vectors have been locked in the array  $W \in \mathbb{C}^{n \times k}$ . At the next iteration, after the filtering step, the QR algorithm then orthogonalizes the matrix  $Z \equiv [W \mathfrak{p}_m(A)V]$ , with  $V \in \mathbb{C}^{n \times (\ell-k)}$ . As before  $\mathfrak{p}_m(A)V$  obeys the spectral decomposition of Equation 2.8 with the only difference that the matrices  $S_{\ell,3}$  have now only  $\ell - k$  columns. For  $W$  we can define the following decomposition

$$(2.11) \quad W = X_\ell Q_\ell + X_3 Q_3 \quad \text{with } Q_\ell \in \mathbb{C}^{\ell \times k} \text{ and } Q_3 \in \mathbb{C}^{(n-\ell) \times k}.$$

Despite the similarities, and because of the convergence check, the matrices  $Q_{\ell,3}$  have quite a different properties than the  $S_{\ell,3}$ . This is because each column vector  $w_i \in W$  satisfies the residual equation

$$(2.12) \quad \|r_i\|_2 = \frac{\|Aw_i - \tilde{\lambda}_i w_i\|_2}{\|w_i\|_2} < \text{TOL}.$$

Moreover it is guaranteed [22][Sec-4.5] that each eigenvalue  $\lambda_i$  lies in a interval defined by the computed eigenvalue  $\tilde{\lambda}_i$  and the residual if the eigenvalues satisfy the uniform separation condition. In other words, if all interval  $[\tilde{\lambda}_i - \|r_i\|_2, \tilde{\lambda}_i + \|r_i\|_2]$  are disjoint, it is guaranteed that  $\tilde{\lambda}_i$  provide a unique approximation to  $\lambda_i$ <sup>2</sup>.

<sup>1</sup>in ChASE the initial vectors  $V^{(0)}$  are chosen to be randomly generated and orthonormal, the vectors  $V^{(i)}$  are by construction orthonormal and typically have a large overlap with the filtered subspace

<sup>2</sup>The case of clustered eigenvalues requires a bit more work and knowledge of the residual matrix of the clustered eigenvalues (see [22][Sec-11.5])

PROPOSITION 2.4. *Under the assumption that each eigenpairs  $(w_i, \tilde{\lambda}_i)$   $i = 1, \dots, k$  satisfies the uniform separation condition and its residual  $\|r_i\| < \text{TOL}$ ,  $\exists \zeta_i = \min_{j \neq i} |\lambda_j - \lambda_i|$  such that  $\forall j \neq i$*

$$\|(Q_\ell)_{:\neq i, i}^2\|_2^2, \|(Q_3)_{:\neq i, i}^2\|_2^2 \leq \left(\frac{\text{TOL}}{\zeta_i}\right)^2$$

*Proof.* Let us write  $A$  in terms of its spectral decomposition  $A = X\Lambda X^H$  and use the decomposition of  $w_i = X_\ell(Q_\ell)_{:,i} + X_3(Q_3)_{:,i}$ , then the numerator of equation (2.12) becomes

$$\begin{aligned} \|Aw_i - \tilde{\lambda}_i w_i\|_2 &= \left[ \sum_{\substack{j=1 \\ j \neq i}}^{\ell} (\lambda_j - \tilde{\lambda}_i)^2 |Q_\ell|_{j,i}^2 + (\lambda_i - \tilde{\lambda}_i)^2 |Q_\ell|_{i,i}^2 + \sum_{j=1}^{n-\ell} (\lambda_j - \tilde{\lambda}_i)^2 |Q_3|_{j,i}^2 \right]^{\frac{1}{2}} \\ &\geq \left[ \sum_{\substack{j=1 \\ j \neq i}}^{\ell} (\lambda_j - \tilde{\lambda}_i)^2 |Q_\ell|_{j,i}^2 + \sum_{j=1}^{n-\ell} (\lambda_j - \tilde{\lambda}_i)^2 |Q_3|_{j,i}^2 \right]^{\frac{1}{2}} \geq \zeta_i \left[ \sum_{\substack{j=1 \\ j \neq i}}^{\ell} |Q_\ell|_{j,i}^2 + \sum_{j=1}^{n-\ell} |Q_3|_{j,i}^2 \right]^{\frac{1}{2}}. \end{aligned}$$

Assuming that  $w_i$  is normalized to Unity, the last inequality directly translates into

$$\left(\frac{\text{TOL}}{\zeta_i}\right)^2 \geq \|(Q_\ell)_{:\neq i, i}^2\|_2^2 + \|(Q_3)_{:\neq i, i}^2\|_2^2$$

proving the statement of the proposition.  $\square$

For all practical purpose,  $|\lambda_{\ell+j} - \tilde{\lambda}_i| \gg \zeta_i$  when  $k < \ell$ , which implies that  $\left(\frac{\text{TOL}}{\zeta_i}\right)^2 \gg \|(Q_3)_{:\neq i, i}^2\|_2^2$ . It is then reasonable to assume that  $W \approx X_\ell Q_\ell$ . Let's separate the subspace of size  $\mathcal{X}_\ell = \mathcal{R}(X_\ell)$  in two parts spanned by the first  $k$  eigenvectors  $X_1$ , corresponding to the number of locked vectors, and the remaining part spanned by  $\ell - k$  eigenvectors  $X_2$ . Then,  $Q_\ell = (Q_1^\top \ Q_2^\top)^\top$  and similarly  $S_\ell = (S_1^\top \ S_2^\top)^\top$  with  $S_1 \in \mathbb{C}^{k \times (\ell-k)}$  and  $S_2 \in \mathbb{C}^{(\ell-k) \times (\ell-k)}$ . The decomposition of  $W$  and  $V$  are simply re-written as

$$W = X_1 Q_1 + X_2 Q_2 \quad \text{and} \quad V = X_1 S_1 + X_2 S_2 + X_3 S_3.$$

REMARK: *In the ChASE Algorithm 1.1, as soon as a number of vectors  $W$  are deflated and locked, they are also made orthogonal by construction to the new array of vector  $V$  that is the new output of the Chebyshev filter and the next subspace iteration. This implies that  $\|W^H V\|_2 = \|Q_1^H S_1 + Q_2^H S_2\|_2 \leq \mathcal{O}(\epsilon^\perp)$  with  $\epsilon^\perp$  the orthogonality accuracy achieved during the Rayleigh-Ritz step. By construction, both  $Q_1$  and  $S_2$  are supposed to be full rank which implies that  $\|Q_2\|_2, \|S_1\|_2 \sim \mathcal{O}(\epsilon^\perp)$ . This is an operational result and it depends on the orthogonality achieved by the direct/dense eigensolver used in the Rayleigh-Ritz step.*

Assuming the validity of the operational remark above, we can finally write the collection of vectors in  $Z$  in the following fashion

$$(2.13) \quad Z = [W \ \text{p}_m(A)V] = \left[ X_1 Q_1 \quad \left( X_2 + X_3 \Gamma_3^m S_3 (S_2)^{-1} (\Gamma_2^m)^{-1} \right) \Gamma_2^m S_2 \right].$$

**3. Bounding the condition number of an array of filtered vectors.** In this section, we build on the spectral decomposition introduced in Sec. 2 to derive a sequence of theorems and propositions that provide upper bounds for the condition number of  $\text{p}_m(A)V$ . We begin by examining the simpler setting in which the same polynomial degree  $m$  is applied uniformly to all vectors in  $V$ . We then extend the analysis to the more general case where the polynomial degree is optimized individually for each filtered vector. Finally, we present a general expression for estimating the condition number in the practical scenario where some vectors have already converged and are therefore deflated and locked.

### 3.1. Single polynomial degree and no locking mechanism.

LEMMA 3.1. *Given the definition of the matrix elements in the spectral decomposition of equation (2.8) the following expressions hold:*

1.  $\kappa_2(X_\ell \Gamma_\ell^m) = \kappa_2(\Gamma_\ell^m) = \frac{|\rho_1|_m}{|\rho_\ell|_m}$
2.  $\kappa_2(S_\ell) = 1$

3.  $\|\Gamma_\ell^m S_\ell\|_2 \leq 1$
4.  $\|S_\ell^+ (\Gamma_\ell^m)^{-1}\|_2 \leq \frac{|\rho_1|^m}{|\rho_\ell|^m}$

*Proof.* The condition number of a general rectangular matrix  $M$  is defined through the pseudo-inverse  $M^+$  as  $\text{cond}_p(M) \doteq \|M\|_p \|M^+\|_p$ . Specifically, when using the 2-norm ( $p = 2$ ),  $\kappa_2(M) = \frac{\sigma_{\max}(M)}{\sigma_{\min}(M)}$  with  $\sigma_{\max}(M)$  and  $\sigma_{\min}(M)$  being the largest and smallest non-zero singular values of  $M$ .

With the above definition in hand, each statement of the Lemma can be derived in few passages.

1. Since  $X_\ell$  is a unitary matrix by definition,  $\|X_\ell \Gamma_\ell^m\|_2 = \|\Gamma_\ell^m\|_2$  and

$$\kappa_2(X_\ell \Gamma_\ell^m) = \kappa_2(\Gamma_\ell^m) = \frac{\sigma_1(\Gamma_\ell^m)}{\sigma_\ell(\Gamma_\ell^m)} = \frac{|\rho_1|^m}{|\rho_\ell|^m}.$$

2. Using the definition of  $S_\ell$ ,  $\kappa_2(S_\ell) = \|X_\ell^H V\|_2 \|(X_\ell^H V)^{-1}\|$ . Because  $V$  is by construction either i. i. d. (at subspace iteration 0) or orthonormal (at later subspace iterations),  $\|X_\ell V\|_2 = \|V\|_2 = 1$ . the same conclusion hold for the norm of the inverse of  $S_\ell$ .
3. The third statement follows from a simple chain of relations

$$\|\Gamma_\ell^m S_\ell\|_2 \leq \|\Gamma_\ell^m\|_2 \|S_\ell\|_2 = \|\Gamma_\ell^m\|_2 = \sigma_{\max}(\Gamma_\ell^m) = 1,$$

where we have used the Schwarz inequality, the intermediate results from statement 2., and the definition of  $\Gamma$ s in equation (2.9) whose values are in descending order from left to right.

4. Similarly to the previous statement, also the last one is deduced by a simple chain of inequalities

$$\|S_\ell^+ (\Gamma_\ell^m)^{-1}\|_2 \leq \|S_\ell^+\|_2 \|(\Gamma_\ell^m)^{-1}\|_2 = \|(\Gamma_\ell^m)^{-1}\|_2 = \frac{|\rho_1|^m}{|\rho_\ell|^m}. \quad \square$$

While simple, the results of the Lemma above are particularly relevant in the case  $p = 2$  norm thanks to the following inequality which holds for two rectangular matrices  $A$  and  $B$  with congruent dimensions

$$(3.1) \quad \kappa_2(AB) \leq \kappa_2(A) \kappa_2(B).$$

For instance, from the 3. and 4. statements and the definition of condition number, it automatically holds that  $\kappa_2(\Gamma_\ell^m S_\ell) \leq \frac{|\rho_1|^m}{|\rho_\ell|^m}$ . Moreover, we can now state and demonstrate the proposition below.

**PROPOSITION 3.2.** *Given a square Hermitian matrix  $A$ , we filter an array of orthonormal vectors  $V$  by a Chebyshev polynomial of degree  $m$  defined by  $p_m(A)$ . For a given  $m$ , the subspace filtered by the polynomial can be built such that  $1 < |\rho_\ell|^m < 1 + \sqrt{2}$ , then the following inequality holds for a constant  $\eta > 1$*

$$(3.2) \quad \kappa_2(p_m(A)V) \leq \eta |\rho_1|^m$$

*Proof.* For the sake of simplicity, let us define  $E^m \doteq \Gamma_3^m S_3 (S_\ell)^{-1} (\Gamma_\ell^m)^{-1}$  and write again Equation (2.8) as

$$p_m(A)V = (X_\ell + X_3 E^m) \Gamma_\ell^m S_\ell$$

In the large  $m$  limit we expect  $X_\ell + X_3 E^m \rightarrow X_\ell$ . For some finite, but large enough values of  $m$ , one can treat the expression  $X_3 E^m$  as a perturbation of  $X_\ell$  and write  $X_3 E^m = -\delta X_\ell$ , such that

$$p_m(A)V = (\mathbb{1} - \delta X_\ell X_\ell^H) X_\ell \Gamma_\ell^m S_\ell = (\mathbb{1} - D) X_\ell \Gamma_\ell^m S_\ell.$$

From Equation (3.1) follows that

$$\kappa_2(p_m(A)V) \leq \kappa_2(\mathbb{1} - D) \kappa_2(X_\ell \Gamma_\ell^m S_\ell) \leq \kappa_2(\mathbb{1} - D) \frac{|\rho_1|^m}{|\rho_\ell|^m}.$$

Following the definition of condition number  $\kappa_2(\mathbb{1} - D) = \|(\mathbb{1} - D)\|_2 \|(\mathbb{1} - D)^{-1}\|_2$ , we need to obtain bounds for the 2-norms on the RHS. From the triangle inequality  $\|\mathbb{1} - D\|_p \leq 1 + \|D\|_p$ , while from Lemma 2.3.3 of Golub Van-Loan (3rd edition) [17] one has that  $\|(\mathbb{1} - D)^{-1}\|_p \leq (\mathbb{1} - \|D\|_p)^{-1}$  if  $\|D\|_p < 1$ . All is left to do is to derive a bound for the norm  $D$ . It useful to express the latter in explicit form

$$-D = X_3 \Gamma_3^m S_3 S_\ell^{-1} (\Gamma_\ell^m)^{-1} X_\ell^H = (X_3 \Gamma_3^m X_3^H) V V^H (X_\ell \Gamma_\ell^m X_\ell^H)^{-1},$$

where in the last equality we have used the definition of the  $S$  matrices. Taking the norm of  $D$  and using successively the triangle inequality and the results from Lemma 3.1, we obtain the following inequality

$$\|D\|_2 \leq \|X_3 \Gamma_3^m X_3^H\|_2 \|V V^H\|_2 \|(X_\ell \Gamma_\ell^m X_\ell^H)^{-1}\|_2 \leq \|\Gamma_3^m\|_2 \|(\Gamma_\ell^m)^{-1}\|_2 = |\rho_\ell|^{-m}.$$

By assumption,  $|\rho_\ell|^m$  is always a number larger than 1, then we can plug in this last result into the definition of  $\kappa_2(\mathbb{1} - D)$  and obtain

$$(3.3) \quad \kappa_2(\mathbb{p}_m(A)V) \leq \frac{|\rho_1|^m}{|\rho_\ell|^m} \cdot \frac{|\rho_\ell|^m + 1}{|\rho_\ell|^m - 1}.$$

Under the condition of the proposition  $\eta \doteq \frac{|\rho_\ell|^m + 1}{|\rho_\ell|^m (|\rho_\ell|^m - 1)} > 1$  which completes the proof.  $\square$

REMARK: In practical cases,  $|\rho_\ell|^m$  is always a number larger than unity but almost never larger than 2. This is because the choice of subspace is such that the eigenvalue  $\lambda_\ell$  is quite close to the extreme of the filtered interval of the spectrum but always included in it. The latter condition guarantee that  $|\rho_\ell|^m > 1$  while its closeness to extreme ensure that it is never too large and always much smaller than  $|\rho_1|^m$ . For this reason, the parameter  $\eta$  is bigger than one but not by too much. We will see in the set of numerical experiments that it is fairly safe to choose the  $\eta = 1$  and use a simplified version of the bound.

**3.2. Optimized polynomial degree.** As we have seen at the end of Section 2.2, when the polynomial degree is optimized  $m$  becomes a vector of size  $\ell$  holding increasingly larger integer values as the vector index grows. In this case Lemma 3.1 can be easily generalized by adding a simple condition.

LEMMA 3.3. Given the definition of the matrix elements in the spectral decomposition of equation (2.8) with the  $\Gamma$ 's expressed by Equation 2.10, and the additional condition that  $|\rho_i|^{m_i} |\rho_1|^{(m_{i+1} - m_i)} \geq |\rho_{i+1}|^{m_{i+1}}$  the following expressions hold:

1.  $\kappa_2(X_\ell \Gamma_\ell^m) = \kappa_2(\Gamma_\ell^m) = \frac{|\rho_1|^{m_\ell}}{|\rho_\ell|^{m_\ell}}$
2.  $\kappa_2(S_\ell) = 1$
3.  $\|\Gamma_\ell^m S_\ell\|_2 \leq 1$
4.  $\|S_\ell^+ (\Gamma_\ell^m)^{-1}\|_2 \leq \frac{|\rho_1|^{m_\ell}}{|\rho_\ell|^{m_\ell}}$

*Proof.* The proof for statements 2. and 3. is exactly the same as for Lemma 3.1. The only difference for the remaining statements is in the structure of the  $\Gamma$ s. As long as the additional condition of the Lemma holds, the values of the diagonal elements of the  $\Gamma$ s are still written in descending ordered so that the same steps in the proof leads to the stated results.  $\square$

A similar result is obtained for Proposition 3.2 where now  $m \rightarrow m_\ell$ . The end results is that, under the condition that  $1 < |\rho_\ell|^{m_\ell} < 1 + \sqrt{2}$ ,

$$(3.4) \quad \kappa_2(\mathbb{p}_m(A)V) \leq \eta |\rho_1|^{m_\ell}$$

with  $\eta \doteq \frac{|\rho_\ell|^{m_\ell} + 1}{|\rho_\ell|^{m_\ell} (|\rho_\ell|^{m_\ell} - 1)} > 1$ . The proof of the statement follows exactly the same steps described in the proof of Proposition 3.2 are not worth repeating here. The clue point is to recognize that the norm of the matrix  $\|D\| \leq |\rho_\ell|^{m_\ell}$ . Similarly to Remark 3.1, as long as the value of  $m_\ell$  is  $\mathcal{O}(10)$ ,  $|\rho_\ell|^{m_\ell}$  is a number larger than 1 but still of  $\mathcal{O}(1)$  and for all practical purposes it can be ignored.

**3.3. Locking and deflating the vectors.** In this case bounding from above the condition number of  $V$  is a bit more complex and requires understanding how the condition number of the spectral decomposition illustrated in Equation (2.13) is influenced by its components. Before attempting a rigorous analysis it is worth making a simple hand waving consideration. The first  $k$  columns of the array  $Z$  are made by a very well behaved sub-array,  $X_1 Q_1$ , whose condition number is by construction likely to be as close to unity as it gets. In fact, this array represents the portion of  $Z$  that has converged and has been deflated. Conversely the sub-array  $(X_2 \Gamma_2^m S_2 + X_3 \Gamma_3^m S_3)$  encloses the part of  $Z$  that may be problematic. As such, one would expect only this part to contribute to the condition number of  $Z$ . In order to show this more rigorously, we state and demonstrate the following proposition.

THEOREM 3.4. Given two rectangular matrices  $A$  and  $B$  with  $A \in \mathbb{C}^{n \times q}$  and  $B \in \mathbb{C}^{n \times p}$ ,  $n > q + p$  and  $A^H B = 0$  (or equivalently  $B^H A = 0$ ), the condition number of  $M \doteq [A \ B] \in \mathbb{C}^{n \times \ell}$  is

$$(3.5) \quad \kappa_2(M) \leq \frac{\sigma_1(A) + \sigma_1(B)}{\inf\{\sigma_q(A), \sigma_p(B)\}}$$

*Proof.* By definition, the condition number of  $M$  is

$$\kappa_2(M) = \|M\|_2 \|M^+\|_2 = \frac{\sigma_1(M)}{\sigma_\ell(M)}$$

where, as before,  $M^+$  indicates the pseudo-inverse of  $M$  and  $\ell = q + p$ . The series of inequalities below hold

$$\sigma_1(M) = \|M\|_2 = \sqrt{\lambda_1(MM^H)} = \|AA^H + BB^H\|_2 \leq \|AA^H\|_2 + \|BB^H\|_2 = \sigma_1(A) + \sigma_1(B)$$

where  $\lambda_1$  and  $\sigma_1$  are respectively the largest eigenvalue and the largest singular value. The norm of the pseudo-inverse is a bit trickier. Since  $M$  has  $\ell$  independent columns the definition of pseudo-inverse is  $M^+ = (M^H M)^{-1} M^H$ . In block forms this becomes

$$\begin{aligned} M^+ &= \left[ \begin{pmatrix} A^H \\ B^H \end{pmatrix} (A \ B) \right]^{-1} \begin{pmatrix} A^H \\ B^H \end{pmatrix} = \begin{pmatrix} A^H A & 0 \\ 0 & B^H B \end{pmatrix}^{-1} \begin{pmatrix} A^H \\ B^H \end{pmatrix} \\ &= \begin{pmatrix} (A^H A)^{-1} A^H & 0 \\ 0 & (B^H B)^{-1} B^H \end{pmatrix} = \begin{pmatrix} A^+ & 0 \\ 0 & B^+ \end{pmatrix} \end{aligned}$$

where we used the proposition assumption in the first step, and the fact that the inverse of block diagonal matrices are equal to the inverse of the blocks in the second step. With this expression we can now easily show that

$$\begin{aligned} [\sigma_\ell(M)]^{-1} &= \sigma_1(M^+) = \left\| \begin{pmatrix} A^+ & 0 \\ 0 & B^+ \end{pmatrix} \right\|_2 \leq \sup\{\|A^+\|_2, \|B^+\|_2\} = \sup\{\sigma_1(A^+), \sigma_1(B^+)\} \\ &= \sup\{\sigma_q(A)^{-1}, \sigma_p(B)^{-1}\} = [\inf\{\sigma_q(A), \sigma_p(B)\}]^{-1} \end{aligned}$$

The central inequality can be derived by using the definition of matrix norm  $\|M^+\|_2 = \sup_{\|v\|=1} \|M^+ v\|_2$  with a vector  $v$  defined as

$$v = \begin{pmatrix} ax \\ by \end{pmatrix} \quad \text{with} \quad a^2 + b^2 = 1 \quad \text{and} \quad \|x\| = \|y\| = 1$$

such that

$$\|M^+\|_2^2 = a^2 \sup \|A^+ x\|_2^2 + b^2 \sup \|B^+ y\|_2^2 \leq (a^2 + b^2) \sup\{\|A^+\|_2^2, \|B^+\|_2^2\} = \sup\{\|A^+\|_2, \|B^+\|_2\}^2 \quad \square$$

The statement of [Theorem 3.4](#) can be directly applied to the  $Z$  matrix of [\(2.13\)](#), with  $M = Z$ ,  $A = X_1 Q_1$  and  $B = X_2 \Gamma_2^m S_2 + X_3 \Gamma_3^m S_3$  and correspondingly  $q = k$  and  $p = \ell - k$ . Because  $A = X_1 Q_1$  represents the array of deflated and locked vectors, it is a unitary matrix by construction. As such,  $\sigma_k(X_1 Q_1) \sim \sigma_1(X_1 Q_1) = \|X_1 Q_1\|_2 = 1$ . Conversely

$$\begin{aligned} \sigma_{\ell-k}^2(B) &= \lambda_{\ell-k} (S_2^H (\Gamma_2^m)^H \Gamma_2^m S_2 + S_3^H (\Gamma_3^m)^H \Gamma_3^m S_3) = \inf_{\|v\|_2=1} v^H (S_2^H (\Gamma_2^m)^H \Gamma_2^m S_2 + S_3^H (\Gamma_3^m)^H \Gamma_3^m S_3) v \\ &= \inf_{\|v\|_2=1} (v^H S_2^H (\Gamma_2^m)^H \Gamma_2^m S_2 v) + \inf_{\|v\|_2=1} (v^H S_3^H (\Gamma_3^m)^H \Gamma_3^m S_3 v) \\ &= \inf_{\|z\|_2=1} (z^H (\Gamma_2^m)^H \Gamma_2^m z) + \inf_{\|u\|_2=1} (u^H S_3^H (\Gamma_3^m)^H \Gamma_3^m S_3 u) = \sigma_{\ell-k}^2(\Gamma_2^m) + \sigma_{n-\ell}^2(\Gamma_3^m) \end{aligned}$$

Since  $\Gamma_2^m$  and  $\Gamma_3^m$  are positive definite and  $\sigma_{\ell-k}(\Gamma_2^m) = \frac{|\rho_\ell|^{m\ell}}{|\rho_1|^{m\ell}} \ll 1$  and  $\sigma_{n-\ell}(\Gamma_3^m) = \frac{1}{|\rho_1|^{m\ell}} \ll 1$  then

$$\sigma_{\ell-k}(\Gamma_2^m S_2 + \Gamma_3^m S_3) \leq \sigma_{\ell-k}(\Gamma_2^m) + \sigma_{n-\ell}(\Gamma_3^m) \ll 1.$$

Similarly, it can be argued that  $\sigma_1((\Gamma_2^m S_2 + \Gamma_3^m S_3)) \gg 1$ . Putting all the pieces together one arrives at

$$\kappa_2(Z) \leq \frac{1 + \sigma_1((\Gamma_2^m S_2 + \Gamma_3^m S_3))}{\sigma_{\ell-k}(\Gamma_2^m S_2 + \Gamma_3^m S_3)} \approx \kappa_2(\Gamma_2^m S_2 + \Gamma_3^m S_3)$$

COROLLARY 3.5. *Given the polynomial filter  $p_m(A)$  of degree  $m$  generated by a square Hermitian matrix  $A$ , and a subspace  $Z$  made by the union of the deflated and locked subspace  $W$  and the filtered subspace  $p_m(A)V$  the following inequality holds for  $1 < |\rho_\ell|^{m_\ell} < 1 + \sqrt{2}$  and a constant  $\eta > 1$*

$$(3.6) \quad \kappa_2(Z) \lesssim \eta |\rho_{k+1}|^{m_{k+1}} |\rho_1|^{m_\ell - m_{k+1}}$$

*Proof.* The proof of the corollary follows exactly the same steps of [Proposition 3.2](#). We start from the [\(3.3\)](#) write the condition number as a product of condition numbers

$$\kappa_2(\Gamma_2^m S_2 + \Gamma_3^m S_3) \leq \kappa_2(\mathbb{1} - D) \kappa_2(X_2 \Gamma_2^m S_2)$$

with the only difference that now  $D = X_3 \Gamma_3^m S_3 S_2^{-1} (\Gamma_2^m)^{-1} X_2^H$ . Because the locking and deflation mechanism,  $\Gamma_2^m$  has a different asymptotic form than  $\Gamma_\ell^m$ , namely

$$\Gamma_2^m = \text{diag}\left(\frac{|\rho_{k+1}|^{m_{k+1}}}{|\rho_1|^{m_{k+1}}}, \dots, \frac{|\rho_\ell|^{m_\ell}}{|\rho_1|^{m_\ell}}\right).$$

Consequently  $\|D\|_2$  can be bound from above by  $|\rho_\ell|^{-m_\ell}$  as in [3.2](#) while

$$\kappa_2(X_2 \Gamma_2^m S_2) \leq \frac{|\rho_{k+1}|^{m_{k+1}} |\rho_1|^{m_\ell - m_{k+1}}}{|\rho_\ell|^{m_\ell}}$$

Putting everything together results in

$$(3.7) \quad \kappa_2(Z) \lesssim \kappa_2(\Gamma_2^m S_2 + \Gamma_3^m S_3) \leq \frac{|\rho_\ell|^m + 1}{|\rho_\ell|^m (|\rho_\ell|^m - 1)} \cdot |\rho_{k+1}|^{m_{k+1}} |\rho_1|^{m_\ell - m_{k+1}}.$$

Once again, under the condition of the corollary one can define  $\eta \doteq \frac{|\rho_\ell|^m + 1}{|\rho_\ell|^m (|\rho_\ell|^m - 1)} > 1$  which completes the proof.  $\square$

**4. Numerical experiments.** The numerical behavior and the benchmark of ChASE has been performed on the cluster JURECA-DC at Jülich Supercomputing Centre in Germany, which has 480 standard homogeneous compute nodes. Each node is equipped two 64 cores AMD EPYC 7742 CPUs @ 2.25 GHz (16 × 32 GB DDR4 Memory), and the interconnects are InfiniBand HDR100 Mellanox Connect-X6. ChASE has been compiled with the default software stack on JURECA-DC. The C/C++ compiler is GCC 13.3.0, the MPI library is OpenMPI 5.0.5, and the BLAS/LAPACK libraries are Intel MKL 2024.2.0.

For the tests on JURECA-DC, the number of MPI ranks per node and OpenMP threads per rank are respectively 4 and 32. The threshold tolerance for residuals `tol` is fixed as  $10^{-10}$ , and the degree optimization of ChASE filter is always enabled unless otherwise specified. All tests in this paper are performed in double-precision.

**4.1. Parallel Scheme in ChASE.** ChASE employs a hybrid parallelization strategy tailored to efficiently handle large-scale eigenproblems on distributed-memory systems. The Chebyshev filter is applied on a 2D MPI process grid, with the number of processes chosen to form a nearly square grid whenever possible, which is preferred to balance communication and computation. The filtering procedure exploits the Hermitian or symmetric structure of the target matrix to optimize the matrix–matrix multiplication kernel. Depending on the polynomial degree of the filter, this operation may involve collective allreduce operations either along the row or column communicators of the 2D grid.

The QR factorization within ChASE, in contrast, is performed on a 1D column communicator derived from the 2D grid. Each column communicator contains a subset of MPI processes corresponding to a vertical partition of the matrix. Within each communicator, the QR factorization is executed in parallel, while the resulting factorization is redundant across different column communicators.

Such a separation of parallelism—2D for filtering, 1D for QR—ensures that both the computationally dominant filter and the numerically critical QR factorization achieve high efficiency. The chosen scheme also naturally accommodates the optimized filter profile based on the matrix structure. For further details on the parallel design, implementation choices, and the reasoning behind the column-redundant QR, we refer the reader to [\[37\]](#).

**4.2. Test Matrix Suite: DFT and BSE matrices.** For the numerical test and benchmarks, we make use of a collection of eigenproblems coming from domain applications. Essential details of these problems are listed in Table 4.1, including a short acronym, the size, the number of eigenpairs sought after, the size of extra searching space used in ChASE, the application software used to extract them, the type of each problem, *nev*—the number of eigenpairs to compute required from real world applications, and *nex*—the size of external searching space.

The FLEUR problems are generated by the FLEUR code [35], which implements a full-potential linearized augmented plane wave (FLAPW) all-electron method. In this approach, the wavefunctions are expanded using augmented plane waves inside muffin-tin spheres and plane waves in the interstitial region, leading to a highly accurate but computationally intensive basis set. In contrast, the FHI-aims DFT calculations [6] employ numeric atom-centered orbitals (NAOs) as basis functions, which are strictly localized around atoms and enable efficient evaluation of integrals. This results in Hamiltonian and overlap matrices with different spectral properties compared to FLAPW-based FLEUR matrices. Specifically, FHI-aims matrices tend to have smaller bandwidth and more clustered eigenvalues due to the local nature of the orbitals, whereas FLEUR matrices are typically denser and have more evenly distributed eigenvalues across the spectrum.

The BSE UIUC problems are obtained from a fork of the Jena BSE code developed at the University of Illinois Urbana-Champaign [39], which builds on the underlying DFT Hamiltonians to compute electron-hole excitations. These problems typically exhibit a clustered spectrum of eigenvalues corresponding to low-energy excitations, which poses distinct challenges for iterative eigenvalue solvers.

By including eigenproblems from DFT calculations coming two distinct application codes using different discretization schemes, as well as from BSE simulations, the test suite covers a range of spectral characteristics, matrix sizes, and numerical complexities, providing a comprehensive benchmark for evaluating the performance and robustness of ChASE. As the spectra of matrices from FHI-aims and Jena BSE is typically denser and more clustered, it requires a relatively larger searching space *nex* compared to the corresponding *nev* (see Table 4.1).

**4.3. Exact Condition number vs estimated.** In this section, we illustrate the effectiveness of the upper bounds introduced in Section 3 for the condition number of the rectangular matrix filtered by the Chebyshev filter<sup>3</sup>. The test problems considered here are the ones listed in Table 4.1. The results are shown in Fig. 4.1, which compare the estimated condition number  $\kappa_2^{\text{est}}$  against an accurate computation of the condition number  $\kappa_2$  of the filtered matrices at each iteration of ChASE until convergence.

We performed the tests on the JURECA-DC cluster, using 4 nodes. All tests were carried out either with the Chebyshev polynomial degree optimization enabled (*opt*) or disabled (*no-opt*) to highlight how the condition number estimation depends on the optimization mechanism. For *no-opt*, the Chebyshev polynomial degree is fixed to 20 at every iteration. For *opt*, the initial degree is 20 for the first iteration and is dynamically adjusted at later iterations for each filtered vector with a maximal degree capped at 36 to prevent excessive ill-conditioning.

As already defined in the previous sections, given a rectangular matrix  $M$  its condition number  $\kappa_2$  is equal to  $\frac{\sigma_{\max}(M)}{\sigma_{\min}(M)}$ . where  $\sigma_{\max}(M)$  and  $\sigma_{\min}(M)$  represent the maximal and minimal singular values of  $M$ . For this test, the matrix  $M$  is distributed along the column communicator, and its singular values are computed directly via ScaLAPACK parallel SVD routines, specifically PDGESVD and PZGESVD for the real and complex double-precision cases, respectively. The estimated condition number  $\kappa_2^{\text{est}}$  is given, in its most general form by Eq. (1.2), which reduces to  $|\rho_{k+1}|^m$  when the degree optimization is disabled (*no-opt*). The case without deflation and locking (Eq. 1.1) is automatically recovered at the very first 1-2 iterations when no eigenpair has yet converged.

Fig. 4.1 shows that the estimated condition number, with and without degree optimization, always bounds from above the computed condition number, making it an effective and reliable estimate. For many cases, the ratio between the  $\kappa_2^{\text{est}}$  and  $\kappa_2$  is always below 2. For some cases (e.g., *opt* case for AuAg 13k or TiO<sub>2</sub> 12k), this ratio can be larger than  $\mathcal{O}(10^4)$  for a few initial iterations, where no eigenpairs have been locked yet. This may be caused by the facts that the estimates for the parameters  $e$  and  $c$  provided by ChASE could be quite inaccurate for the first 2 to 3 iterations. Independently from its strictness,  $\kappa_2^{\text{est}}$  always bound  $\kappa_2$  from above and so it constitutes a reliable parameter for ChASE to switch from a more stable QR factorization, such as *s*-Cholesky QR factorization, to the less stable but more efficient CholeskyQR2, even CholeskyQR1 in the last one or two iterations where the estimations are  $\mathcal{O}(1)$ .

<sup>3</sup>If some eigenpairs are locked, this should be the union of the locked eigenvectors and the filtered unconverged ones

Table 4.1: List of DFT matrices for numerical tests.

Name	$N$	nev	nex	Problem Type	Code Source	Type
NaCl 9k	9273	256	60	DFT	<b>FLEUR</b>	Hermitian
AuAg 13k	13379	972	100	DFT	<b>FLEUR</b>	Hermitian
TiO2 12k	12455	1076	100	DFT	<b>FLEUR</b>	Hermitian
TiO2 29k	29528	2560	400	DFT	<b>FLEUR</b>	Hermitian
HfO2 62k	62681	100	100	BSE	<b>BSE UIUC</b>	Hermitian
In2O3 76k	76887	120	60	BSE	<b>BSE UIUC</b>	Hermitian
In2O3 115k	115459	2400	1600	BSE	<b>BSE UIUC</b>	Hermitian
Si GRAPHENE 50k	51476	2400	1600	DFT	<b>FHI-aims</b>	Symmetric
Cu2BASNS4 80k	80250	3600	2400	DFT	<b>FHI-aims</b>	Symmetric

In the *no-opt* case, the highest condition number comes at the first iteration. To clarify, in Fig. 4.1, step 0 corresponds to the QR factorization of the randomly generated initial guess vectors, occurring before the first application of the Chebyshev filter. Therefore, if the condition number of  $M$  at the first iteration is below a certain threshold, the *s-CholeskyQR2* can be avoided in any of the following iterations. Conversely, in the *opt* case the condition number of  $M$  at the early stage can be much larger than the one at the first iteration. This effect is caused by the higher maximal degree allowed during the degree optimization procedure and it is controllable by the user by setting a relative smaller maximal degree for the degree optimization. Observe, though, that ChASE with degree optimization can always converge considerably faster than ChASE without degree optimization (e.g., In<sub>2</sub>O<sub>3</sub> 115k). In conclusion, our upper bound estimation of the condition number for the filtered matrix ensure that the proposed heuristic to switch between QR variants is reliable throughout the entire execution cycle of ChASE.

**4.4. ChASE with CholeskyQR vs Householder QR.** In this section, we compare the numerical behavior of ChASE using either a Householder QR (HHQR) factorization at every iteration or the automatic selection of QR variants based on the heuristic introduced in Section 1.3. Here, HHQR refers to the Householder QR implementation provided by ScaLAPACK, executed on a 1D MPI grid independently over each column communicator. The block size for the ScaLAPACK block-cyclic distribution is set to 64. All tests in this section were run on 4 nodes of the JURECA-DC cluster, using all available CPU cores. Each reported value corresponds to the average of 5 repetitions.

The test problems are those listed in Table 4.1. In all cases, the matrix to be factorized has dimensions  $N \times (\text{nev} + \text{nex})$ . Tables 4.2 reports the total number of matrix-vector multiplications (MatVecs)<sup>4</sup>, the number of ChASE iterations to convergence, the total time-to-solution, and the time spent in the QR factorization. The results show that ChASE equipped with CholeskyQR achieves numerically identical convergence compared to HHQR: the number of iterations and MatVec operations remain effectively the same for all test problems. The main difference is in performance: CholeskyQR consistently reduces the time spent in QR factorizations, with speedups ranging from 2-5 $\times$  for moderate problem sizes ( $\text{nev} \lesssim 1000$ ) and up to 4-6 $\times$  for larger problems ( $\text{nev} \gtrsim 2000$ ), leading to a total time-to-solution reduction of 10–20% depending on the problem.

In conclusion, these results confirm that replacing a stable HHQR with CholeskyQR, guided by the condition number bounds introduced in Section 3, preserves the numerical behavior of ChASE while providing substantial computational reduction, particularly for problems with a larger number of desired eigenpairs. Detailed parallel scaling and performance analysis are discussed in the following section.

**4.5. Strong scaling.** We evaluate the strong scaling behavior of ChASE using In<sub>2</sub>O<sub>3</sub> 115k eigenproblem defined in Table 4.1 with three eigenpair configurations: 1) **Small** ( $\text{nev} = 1200$ ,  $\text{nex} = 600$ ); 2) **Medium** ( $\text{nev} = 2400$ ,  $\text{nex} = 1200$ ); 3) **Large** ( $\text{nev} = 3600$ ,  $\text{nex} = 2400$ ). These labels are used consistently throughout the section to distinguish problem sizes. All runs were performed on the JURECA-DC cluster, scaling from 16 up to 100 compute nodes with 4 MPI ranks per node, and 32 OpenMP threads per MPI process.

<sup>4</sup>At each ChASE iteration, the Chebyshev filter is applied to a rectangular matrix  $M$  where each column may use a different polynomial degree. The number of matrix-vector multiplications (MatVecs) is accumulated over all unconverged eigenpairs and all iterations, providing a measure of the computational work in the filter and offering insight into the convergence behavior of individual filtered vectors.

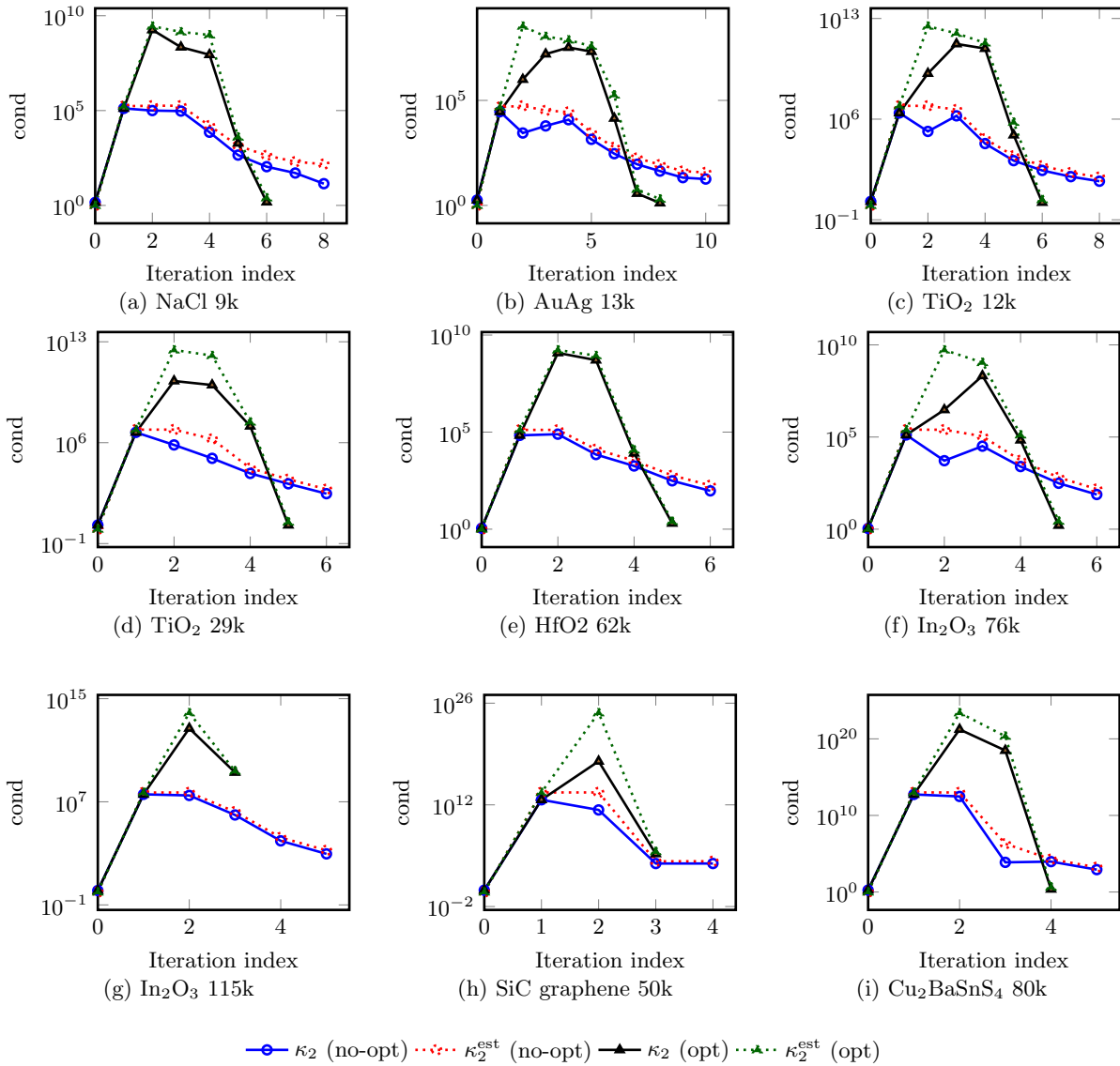


Fig. 4.1: Condition estimates per iteration for various materials with and without optimization. Subplots (a)–(i) show results for different material systems.

The number of nodes in each benchmark is chosen to form a square MPI process grid in ChASE, which is generally preferred for performance.

Figure 4.2 reports both the total time-to-solution and parallel efficiency, along with the time and efficiency specifically for the QR factorization using CholeskyQR and Householder QR. In ChASE, QR is performed only within the column communicator—that is, a subset of the global 2D MPI grid. For instance, in a run employing 64 nodes with 256 MPI processes in total, the column communicator typically spans only 16 MPI processes; hence, the QR timing and efficiency reflect the scaling behavior of this smaller communicator.

The total runtime decreases consistently with increasing MPI process count across all configurations, demonstrating good strong scaling. When CholeskyQR is used, for the smallest case ( $n_{\text{ev}} + n_{\text{ex}} = 1800$ ), the total time drops from approximately 534s on 16 nodes to 124s on 100 nodes. For the largest configuration ( $n_{\text{ev}} + n_{\text{ex}} = 6000$ ), the runtime decreases from about 1890 on 16 nodes to 702s on 100 nodes. Parallel efficiency relative to the smallest node count declines moderately as expected with increased communication overhead: at 100 nodes, it ranges from 0.62-0.72 for the smallest configuration to 0.40-0.43 for the largest one. Notice that the parallel efficiency for medium and large  $n_{\text{ev}}$  degrades more

Table 4.2: Comparison of ChASE-CPU with HHQR and CholeskyQR

Type	QR Impl.	MatVecs	Iters.	All (s)	QR (s)
NaCl 9k	HHQR	34,206	6	8.64	1.34
	CholeskyQR	34,212	6	8.14	0.51
AuAg 13k	HHQR	106,542	8	40.13	8.72
	CholeskyQR	106,618	8	32.96	1.72
TiO2 12k	HHQR	94,724	6	32.47	7.62
	CholeskyQR	93,904	6	26.05	1.92
TiO2 29k	HHQR	212,024	5	323.21	81.56
	CholeskyQR	211,984	5	278.11	16.23
HfO2 62k	HHQR	19,614	5	201.41	5.91
	CholeskyQR	19,614	5	195.33	1.95
In2O3 76k	HHQR	15,980	5	284.62	6.97
	CholeskyQR	15,976	5	278.25	1.81
In2O3 115k	HHQR	229,714	3	2533.05	184.65
	CholeskyQR	229,716	3	2439.24	74.91
Si GRAPHENE 50k	HHQR	240,554	3	263.33	53.98
	CholeskyQR	240,536	3	208.91	8.90
Cu2BASnS4 80k	HHQR	413,084	4	911.62	139.72
	CholeskyQR	429,620	4	747.72	30.11

rapidly since both the QR factorization and Rayleigh-Ritz procedure become more relevant overall and do not scale as nicely as the polynomial filter.

Focusing on the QR factorization, CholeskyQR version consistently outperforms Householder QR across all problem sizes. In the largest configuration ( $nev + nex = 6000$ ), when executed on 20 MPI processes within the column communicator, CholeskyQR completes in 100s compared to 146s for Householder QR, achieving a speedup of roughly  $1.46\times$ . For moderate configurations, the speedup even goes to  $2\text{--}3\times$ , and more the smallest case, this speedup can achieve over  $4\times$ . Since QR is one of the dominant computational components of each ChASE iteration, these reductions in QR time directly contribute to a significant decrease in total runtime, particularly for large eigenproblems.

The parallel efficiency of QR mirrors these improvements. CholeskyQR maintains higher efficiency than Householder QR across all node counts and problem sizes. For instance, in the largest configuration, CholeskyQR retains an efficiency of about 0.79–0.83 on 8–20 MPI processes in the column communicator, while Householder QR efficiency drops more sharply, to approximately 0.53–0.61. This difference reflects the lower communication overhead and simpler computational structure of CholeskyQR, which allows it to scale more effectively within the column communicator even as the number of nodes increases.

Importantly, the convergence behavior of ChASE is essentially unaffected by the choice of QR variants: the total number of iterations and MatVecs remain nearly identical. These results confirm that CholeskyQR variant with heuristic selection can safely replace Householder QR without compromising numerical robustness, while simultaneously delivering higher parallel efficiency, shorter QR execution time, and reduced total time-to-solution.

**5. Summary and conclusions.** In this work, we investigate how to estimate the condition number of a set of vectors  $V$  after they have undergone a transformation through a polynomial filter  $p_m(A)$ . Our study is motivated by the possibility of replacing the traditional Householder-based QR factorization with the more computationally efficient CholeskyQR algorithm. Although CholeskyQR offers improved performance and exposes greater parallelism, it is known to suffer from a loss of orthogonality when the condition number of the matrix of vectors  $p_m(A)V$  becomes too large. To mitigate this issue, one can employ more robust variants such as CholeskyQR2 or, in cases of stronger ill-conditioning, the shifted CholeskyQR2 algorithm. Each of these approaches, however, remains reliable only within specific bounds of the condition number of  $p_m(A)V$ . Consequently, their effective use requires some prior knowledge or estimate of this quantity.

Directly computing the exact condition number of  $p_m(A)V$  would be prohibitively expensive and

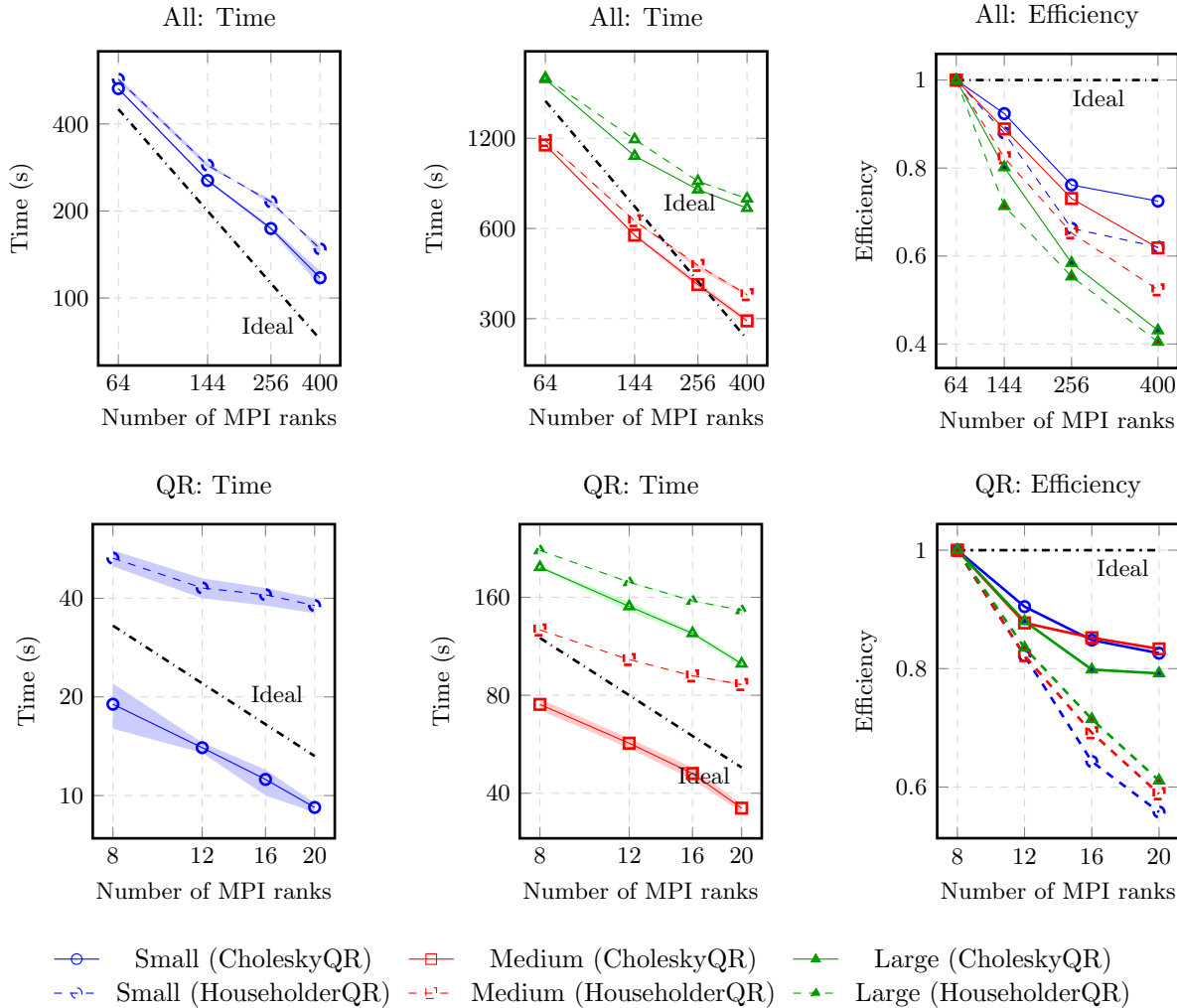


Fig. 4.2: Strong-scaling performance and parallel efficiency comparison between CholeskyQR and Householder QR across configurations. Each measurement was repeated five times. Runtime plots show the average execution time, with shaded bands indicating the minimum–maximum range across runs. Parallel efficiency is computed from the averaged runtimes.

would compromise the performance benefits offered by the CholeskyQR-based methods. In this paper, we therefore address the problem by a careful numerical analysis of the spectral properties of the matrix of filtered vectors. Such analysis lead us to the introduction of a simple and inexpensive estimate of the condition number. The proposed estimate relies only on the convergence ratios of selected column vectors in  $p_m(A)V$  together with the degree  $m_i$  of the polynomial filter applied to them. Based on this estimate, we derive a practical model for dynamically selecting the most appropriate QR factorization variant, thereby maximizing performance and scalability while preserving numerical accuracy. The resulting strategy has been incorporated into version 1.6.0 of the ChASE library and thoroughly validated through numerical experiments.

**Acknowledgements.** This research was in part supported by the Gauss Centre for Supercomputing e.V. ([www.gauss-centre.eu](http://www.gauss-centre.eu)) through the SiVeGCS project and the Joint Lab Virtual Materials Design (JL-VMD), a cross-center platform of the Helmholtz Association established in the Helmholtz Research Field 'Information'. We are thankful to the Jülich Supercomputing Center for the computing time made available to perform the numerical tests. Special thanks to the team members of the Simulation and Data Lab Quantum Materials for insightful discussions and the maintainers of the FLEUR, BSE UIUC and FHI-aims codes for generating and providing the matrices of the eigenproblems used in the numerical tests.

## REFERENCES

- [1] GREY BALLARD, JAMES DEMMEL, LAURA GRIGORI, MATHIAS JACQUELIN, NICHOLAS KNIGHT, AND HONG DIEP NGUYEN, *Reconstructing householder vectors from tall-skinny qr*, Journal of Parallel and Distributed Computing, 85 (2015), pp. 3–31.
- [2] AMARTYA S. BANERJEE, LIN LIN, WEI HU, CHAO YANG, AND JOHN E. PASK, *Chebyshev polynomial filtered subspace iteration in the discontinuous galerkin method for large-scale electronic structure calculations*, The Journal of Chemical Physics, 145 (2016), p. 154101.
- [3] AMARTYA S. BANERJEE, LIN LIN, PHANISH SURYANARAYANA, CHAO YANG, AND JOHN E. PASK, *Two-level chebyshev filter based complementary subspace method: Pushing the envelope of large-scale electronic structure calculations*, Journal of Chemical Theory and Computation, 14 (2018), pp. 2930–2946.
- [4] FRIEDRICH L. BAUER, *Das Verfahren der Treppeniteration und verwandte Verfahren zur Lösung algebraischer Eigenwertprobleme*, Zeitschrift für Angewandte Mathematik und Physik ZAMP, 8 (1957), pp. 214–235.
- [5] MARIO BERLJAJA, DANIEL WORTMANN, AND EDOARDO DI NAPOLI, *An optimized and scalable eigensolver for sequences of eigenvalue problems*, Concurrency and Computation: Practice and Experience, 27 (2015), pp. 905–922.
- [6] VOLKER BLUM, RALF GEHRKE, FELIX HANKE, PAULA HAVU, VILLE HAVU, XINGUO REN, KARSTEN REUTER, AND MATTHIAS SCHEFFLER, *Ab initio molecular simulations with numeric atom-centered orbitals*, Computer Physics Communications, 180 (2009), pp. 2175–2196.
- [7] MAURICE CLINT AND A. JENNING, *The evaluation of eigenvalues and eigenvectors of real symmetric matrices by simultaneous iteration*, The Computer Journal, 13 (1970), pp. 76–80.
- [8] MICHEL CROUZEIX, BERNARD PHILIPPE, AND MILOUD SADKANE, *The Davidson method*, SIAM Journal on Scientific Computing, 15 (1994), pp. 62–76.
- [9] JANE CULLUM AND W DONATH, *A block Lanczos algorithm for computing the q algebraically largest eigenvalues and a corresponding eigenspace of large, sparse, real symmetric matrices*, in 1974 IEEE Conference on Decision and Control including the 13th Symposium on Adaptive Processes, IEEE, 1974, pp. 505–509.
- [10] JANE K CULLUM AND RALPH A WILLOUGHBY, *Lanczos Algorithms for Large Symmetric Eigenvalue Computations Volume 1*, Theory, Birkhauser, 1985.
- [11] ERNEST R DAVIDSON, *The iterative calculation of a few of the lowest eigenvalues and corresponding eigenvectors of large real-symmetric matrices*, Journal of Computational Physics, 17 (1975), pp. 87–94.
- [12] JAMES DEMMEL, LAURA GRIGORI, MARK HOEMMEN, AND JULIEN LANGOU, *Communication-avoiding parallel and sequential qr factorizations*, CoRR abs/0806.2159, (2008).
- [13] EDOARDO DI NAPOLI AND MARIO BERLJAJA, *Block Iterative Eigensolvers for Sequences of Correlated Eigenvalue Problems*, arXiv.org, (2012).
- [14] EDOARDO DI NAPOLI, XINZHE WU, AND CLEMENT RICHEFORT, *The ChASE library*. <https://github.com/ChASE-library/ChASE>, 2026. Accessed:2026-03-10.
- [15] TAKESHI FUKAYA, RAMASESHAN KANNAN, YUJI NAKATSUKASA, YUSAKU YAMAMOTO, AND YUKA YANAGISAWA, *Shifted cholesky qr for computing the qr factorization of ill-conditioned matrices*, SIAM Journal on Scientific Computing, 42 (2020), pp. A477–A503.
- [16] TAKESHI FUKAYA, YUJI NAKATSUKASA, YUKA YANAGISAWA, AND YUSAKU YAMAMOTO, *Choleskyqr2: a simple and communication-avoiding algorithm for computing a tall-skinny qr factorization on a large-scale parallel system*, in 2014 5th workshop on latest advances in scalable algorithms for large-scale systems, IEEE, 2014, pp. 31–38.
- [17] GENE H. GOLUB AND C. F. VAN LOAN, *Matrix Computations*, Johns Hopkins Univ., Baltimore and London, 3rd edition ed., 2012.
- [18] MORITZ KREUTZER, DOMINIK ERNST, ALAN R. BISHOP, HOLGER FEHSKE, GEORG HAGER, KENGO NAKAJIMA, AND GERHARD WELLEIN, *Chebyshev filter diagonalization on modern manycore processors and gpgpus*, in High Performance Computing, Rio Yokota, Michèle Weiland, David Keyes, and Carsten Trinitis, eds., Cham, 2018, Springer International Publishing, pp. 329–349.
- [19] LEEOR KRONIK, ADI MAKMAL, MURILO L TIAGO, M M G ALEMANY, MANISH JAIN, XIANGYANG HUANG, YOUSEF SAAD, AND JAMES R CHELIKOWSKY, *PARSEC – the pseudopotential algorithm for real-space electronic structure calculations: recent advances and novel applications to nano-structures*, physica status solidi (b), 243 (2006), pp. 1063–1079.
- [20] ANTOINE LEVITT AND MARC TORRENT, *Parallel eigensolvers in plane-wave Density Functional Theory*, Computer Physics Communications, 187 (2015), pp. 98–105.
- [21] EDOARDO DI NAPOLI, CLÉMENT RICHEFORT, AND XINZHE WU, *Chebyshev accelerated subspace eigensolver for pseudo-hermitian hamiltonians*, 2026.
- [22] BERESFORD N. PARLETT, *The Symmetric Eigenvalue Problem*, SIAM, Philadelphia, PA, Jan. 1998.
- [23] B N PARLETT AND D S SCOTT, *The Lanczos algorithm with selective orthogonalization*, Mathematics of Computation, 33 (1979), pp. 217–238.
- [24] ALDO H. ROMERO, DOUGLAS C. ALLAN, BERNARD AMADON, GABRIEL ANTONIUS, THOMAS APPLENCOURT, LUCAS BAGUET, JORDAN BIEDER, FRANÇOIS BOTTIN, JOHANN BOUCHET, ERIC BOUSQUET, FABIEN BRUNEAU, GUILAUME BRUNIN, DAMIEN CALISTE, MICHEL CÔTÉ, JULES DENIER, CYRUS DREYER, PHILIPPE GHOSEZ, MATTEO GIANTOMASSI, YANNICK GILLET, OLIVIER GINGRAS, DONALD R. HAMANN, GEOFFROY HAUTIER, FRANÇOIS JOLLET, GÉRALD JOMARD, ALEXANDRE MARTIN, HENRIQUE P. C. MIRANDA, FRANCESCO NACCARATO, GUIDO PETRETTO, NICHOLAS A. PIKE, VALENTIN PLANES, SERGEI PROKHORENKO, TONATIUH RANGEL, FABIO RICCI, GIAN-MARCO RIGNANESE, MIQUEL ROYO, MASSIMILIANO STENGEL, MARC TORRENT, MICHEL J. VAN SETTEN, BENOIT VAN TROEYE, MATTHIEU J. VERSTRAETE, JULIA WIKTOR, JOSEF W. ZWANZIGER, AND XAVIER GONZE, *Abinit: Overview and focus on selected capabilities*, The Journal of Chemical Physics, 152 (2020), p. 124102.
- [25] AXEL RUHE, *Rational Krylov sequence methods for eigenvalue computation*, Linear Algebra and its Applications, 58 (1984), pp. 391–405.
- [26] HEINZ RUTISHAUSER, *Computational aspects of FL Bauer’s simultaneous iteration method*, Numerische Mathematik, 13 (1969), pp. 4–13.

- [27] ———, *Simultaneous iteration method for symmetric matrices*, Numerische Mathematik, 16 (1970), pp. 205–223.
- [28] H. RUTISHAUSER, *Simultaneous iteration method for symmetric matrices*, Handbook for Automatic Computation, (1971).
- [29] YOUSEF SAAD, *Numerical methods for large eigenvalue problems*, SIAM, Philadelphia, PA, 2011.
- [30] G. W. STEWART, *Accelerating the orthogonal iteration for the eigenvectors of a Hermitian matrix*, Numerische Mathematik, 13 (1969), pp. 362–376.
- [31] ———, *Simultaneous iteration for computing invariant subspaces of non-Hermitian matrices*, Numerische Mathematik, 25 (1976), pp. 123–136.
- [32] ———, *Matrix algorithms. Vol. II*, SIAM, Philadelphia, PA, 2001.
- [33] ———, *A Krylov–Schur Algorithm for Large Eigenproblems*, SIAM Journal on Matrix Analysis and Applications, 23 (2002), pp. 601–614.
- [34] J. WINKELMANN, P. SPRINGER, AND E. DI NAPOLI, *ChASE: Chebyshev Accelerated Subspace Iteration Eigensolver for Sequences of Hermitian Eigenvalue Problems*, ACM Transactions on Mathematical Software, 45 (2019), pp. 1–34.
- [35] DANIEL WORTMANN, GREGOR MICHALICEK, NADJIB BAADJI, WEJDAN BEIDA, MARKUS BETZINGER, GUSTAV BIHLMAYER, THOMAS BORNHAKE, JENS BRÖDER, TOBIAS BURNUS, JUSSI ENKOVAARA, ET AL., *Fleur*, Zenodo, (2023).
- [36] K. WU AND H. SIMON, *Thick-restart Lanczos method for large symmetric eigenvalue problems*, SIAM Journal on Matrix Analysis and Applications, (2000).
- [37] X. WU, D. DAVIDOVIĆ, S. ACHILLES, AND E. DI NAPOLI, *Chase: a distributed hybrid cpu-gpu eigensolver for large-scale hermitian eigenvalue problems*, in Proceedings of the Platform for Advanced Scientific Computing Conference, 2022, pp. 1–12.
- [38] XINZHE WU AND EDOARDO DI NAPOLI, *Advancing the distributed multi-gpu chase library through algorithm optimization and nccl library*, in SC-W '23: Proceedings of the SC '23 Workshops of the International Conference on High Performance Computing, Network, Storage, and Analysis, SC-W '23, New York, NY, USA, 2023, Association for Computing Machinery, p. 1688–1696.
- [39] X. ZHANG, S. ACHILLES, J. WINKELMANN, R. HAAS, A. SCHLEIFE, AND E. DI NAPOLI, *Solving the bethe-salpeter equation on massively parallel architectures*, Computer Physics Communications, 267 (2021), p. 108081.
- [40] YUNKAI ZHOU, JAMES R. CHELIKOWSKY, AND YOUSEF SAAD, *Chebyshev-filtered subspace iteration method free of sparse diagonalization for solving the Kohn–Sham equation*, Journal of Computational Physics, 274 (2014), pp. 770–782.
- [41] YUNKAI ZHOU, YOUSEF SAAD, MURILO L. TIAGO, AND JAMES R. CHELIKOWSKY, *Self-consistent-field calculations using Chebyshev-filtered subspace iteration*, Journal of Computational Physics, 219 (2006), pp. 172–184.